OFFSHORE TECHNOLOGY
RESEARCH CENTER

Detection of Deep Water Breaking Waves

by

Charles-Alexandre Zimmermann

AC

A NATIONAL SCIENCE FOUNDATION ENGINEERING RESEARCH CENTER

breaking events according to the video records, in order to find certain characteristic patterns in the frequency signal allowing the identification of breaking events. An example of this wave elevation and frequency signal is shown in Figure 14.

Height parameter

At the beginning, and after looking at this frequency signal, it was very clear that it would be very difficult to identify the breaking events just by using the frequency signal since the peaks were ranged from -100 radians to 100 radians and would not necessarily correspond to breaking waves. In fact, after the careful review of a few experiments, it was noticed that the largest peaks in frequency were corresponding to points where the wave elevation was almost zero. This is in perfect agreement with the results that we obtained in the analysis of the Phase-Time Method in chapter 3.

Therefore, we tried to get rid of this noise in the frequency signal before studying the data further. The most natural way to do this is to implement a filter in the frequency deviation signal. We tried 2 or 3 different simple filters (3, 5 and 7 points filters) on the signal, but the benefits were very limited. If indeed the signal got smoother, the small peaks disappear and the huge peaks corresponding to a zero wave elevation are smaller, they are still present and forbid any meaningful use of the rest of the frequency signal.

In fact, the only way to satisfactorily eliminate this noise is to simply exclude the events of near-zero wave elevations. Since the breaking of a deep water wave will only occur when the wave height is relatively large, the simplest way to get rid of these false

signals was to set an elevation threshold under which the frequency signal would be ignored.

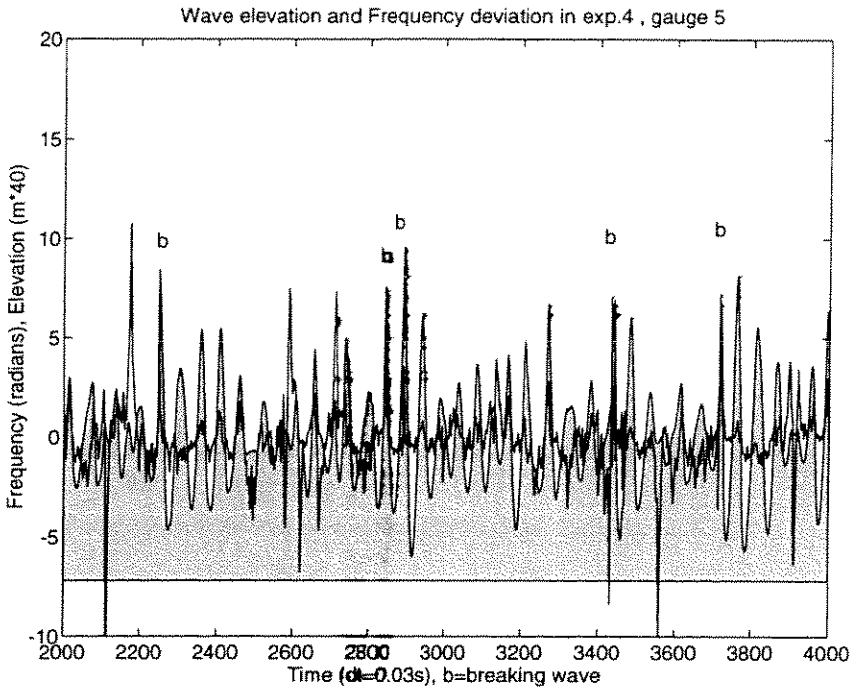

Figure 14. Wave elevation and frequency deviation in experiment 4.

1.5 times the standard deviation (σ) was found to be effective as a threshold for the wave height. It was clear when we checked in the experiment that almost no breaking occurred when the wave height was lower than this limit. When the parameter was implemented in the program, all the huge peaks disappeared, leaving a few corresponding to the biggest waves of the record. This was very encouraging since it changed the frequency signal from a useless signal to a signal that would show some very interesting patterns.

Frequency signal analysis

The next step was to study this frequency signal as a detection tool for the breaking events. Different researchers had focused on this method in the last few years. The comparison of their results to ours will be shown in the next paragraphs.

Since each experiment was conducted using 11 gauges (except the first 3 experiments) and 32700 data points for each of these gauges, it was quite difficult to visualize and try to characterize every pattern in the frequency signal. However by looking at the most important breakers, and incipient breakers for each gauge of different experiments, certain characteristics were found in the frequency signal which correspond to different breakers. First of all, there was a consistent frequency deviation signal corresponding to an incipient breaker. Indeed, the deviation in the local frequency for the initiation of a breaking wave or for an incipient breaker will both provide very high peaks (higher deviation than for the heaviest breaking phases). The frequency signal for all these kind of breakers is very similar, and we can see in Figure 15 the frequency deviation signal for these incipient breakers. This figure shows an average of 50 incipient breaking waves. It was done by aligning the peaks of the frequency deviation for the breaking waves considered and by averaging them. Since the experiments considered for this average were very close in peak period, the shapes of the frequency deviation were not adjusted. This shape is very characteristic of the incipient breaker, and will rarely vary from the figure shown. It is also shown that the large breaking waves will have this

frequency signal shape at the gauge where the breaking will start, and that during the breaking itself, medium or large, this frequency signal will be much less important.

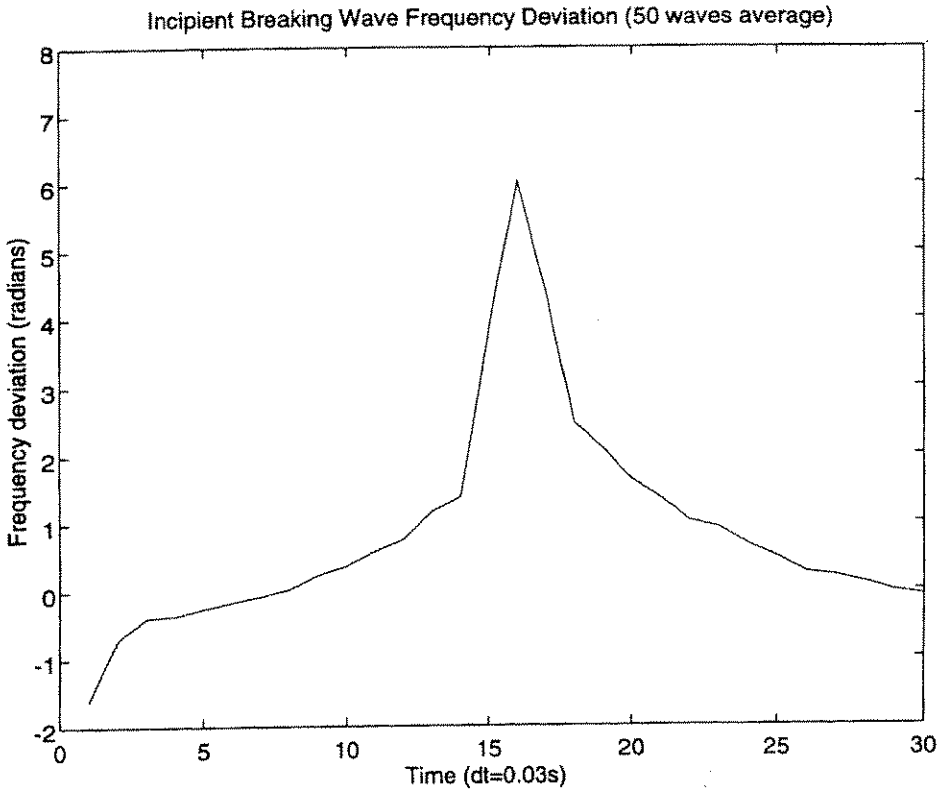

Figure 15. Local frequency deviation for incipient breakers.

Indeed, the frequency signal at the peak of the breaking (i.e. when the white capping is very important, and when the wave is breaking on the front dramatically) will be most of the time very reduced compared to the incipient zone of the breaking. Therefore, the waves that are incipient breakers continuously will have a consistent and high frequency deviation in every gauge crossed by the breaking waves compared to a very short (1 or 2 gauges only) high frequency deviation for the largest breaking waves in the experiment.

This can explain the fact that false detection can occur due to the pattern of certain waves which are very high, sharp, almost breaking, but which do not have enough energy to break. These breakers may also have a high frequency deviation at one point during their evolution, and can be misjudged as a real breaker. However, it is certain that these false breakers could be dismissed by the use of a second gauge next to the first one which would also be used in a detection scheme.

Another important characteristic pattern is the appearance in the frequency signal of "double peak" waves. In some cases, the frequency deviation signal will present a double peak at the point of breaking. The first peak corresponds to the front face of the wave, and the second one to the crest of the wave. This phenomenon will occur for very large breaking waves (almost plunging waves) but is not necessarily present in every large breaker. An averaged shape of this double peak frequency is shown in Figure 16. The method used for the average was the same except the alignment was done on the first peak. This double peak is very interesting and may be explained by the splashing and white capping of water at the front of a large breaker, an obvious location for concentrations of high frequency energy. This double peak was found in every experiment that was conducted and therefore will denote an unusually large breaker whenever it is found in a wave elevation record.

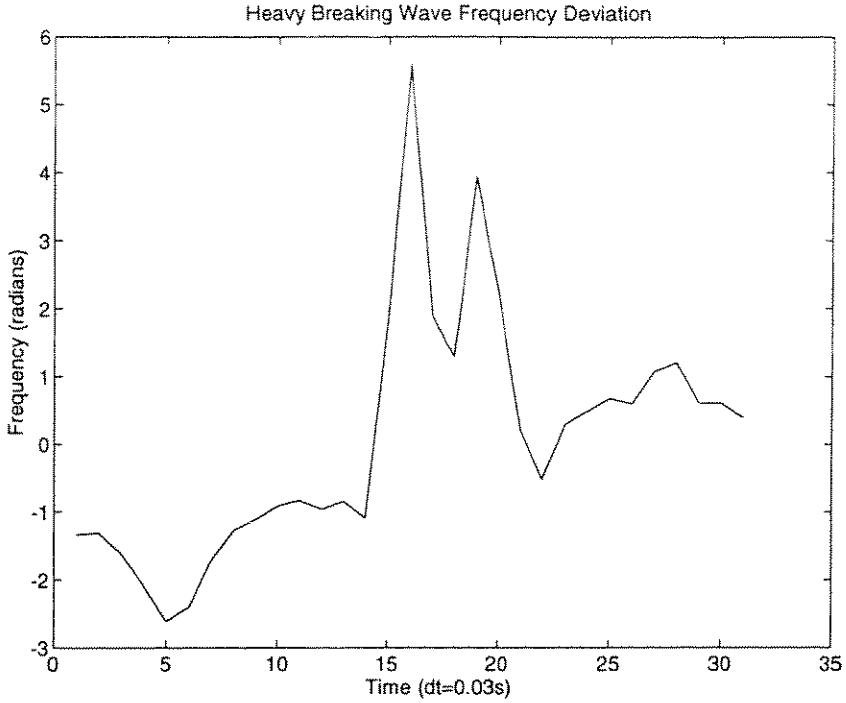

Figure 16. Local frequency deviation for large breakers (double peak shape).

Griffin et. al [1996] studied the patterns of the frequency signal concerning the kinematics and dynamics of deep water breaking waves. In their paper, they show that plunging waves have a much higher frequency deviation than spilling waves. Moreover, in every spilling wave that they studied, the frequency deviation signal increases gradually gauge after gauge and is maximum at the gauge where full breaking occurs. They stated that the evolution of the Hilbert frequency of the packet toward breaking in their wave channel shows nearly constant behavior for the steep but non-breaking waves, slight growth for spilling breakers, and a progression to sharp growth for fully plunging breakers. This is in contradiction with the results found in our experiments, since the higher frequency deviation is most often found at the initiation of the breaking of the

wave. Moreover we found a dissipation of the frequency deviation for the large breakers instead of a progression, and finally many non-breaking waves are detected because of their quite high frequency deviation (therefore no constant behavior). This can be explained mainly by the fact that their experiments involved a concentration of wave packets at one point within their gauge array in order to obtain breaking, whereas our experiment was based on random waves of JONSWAP type spectrum which are created and can break anywhere in the basin (not necessarily within the array of gauges). The waves created and studied in our experiments are closer to ocean waves, and therefore it is more likely that the frequency deviations we studied will be found in the real ocean. Figure 17 shows the evolution of the wave elevation of a large breaking wave (the wave of figure 13) crossing the first 7 gauges in the array. Figure 18 shows the frequency deviation of the same wave for each gauge it crossed. The frequency deviation in Gauge 3 shows a high and sharp peak characteristic of the incipience of a breaker and the deviation in Gauge 5 shows a double peak shape, characteristic of a large breaker. It is obvious in this figure that the frequency deviation signal dissipates with the breaking of the wave.

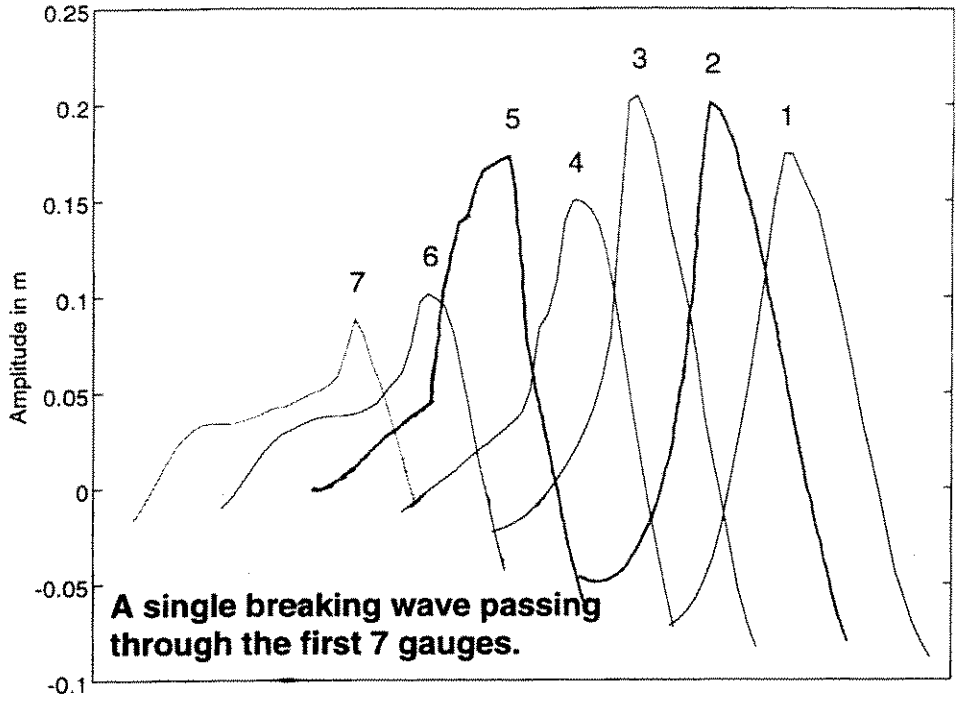

Figure 17. Single breaking wave passing through the 7 first gauges.

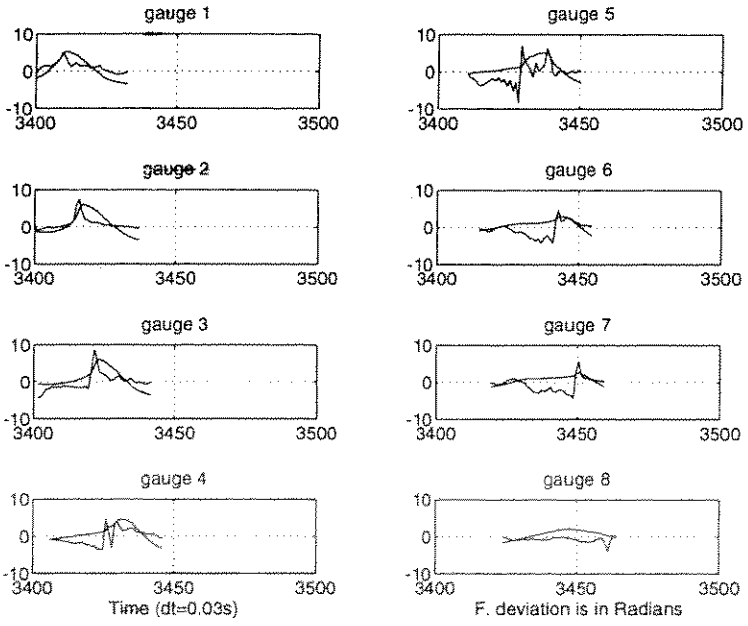

Figure 18. Frequency deviation for the single breaking wave of Figure 17.

After different gauges on one experiment had been studied, it was obvious that the frequency signal obtained in the Phase-Time Method was very useful in detecting the breaking events in the wave elevation records. In fact the frequency signal deviates very rarely for waves that are not breaking, and will always deviate for a breaking wave. It is very difficult to locate exactly a level above which the breaking waves will deviate and the video documentation helped a lot in this matter. In order to have a fresh view of the local frequency deviation of the breaking waves for each experiment, each breaking event that had been noted with the different categories of breaking (I,S,M and L) was associated with its frequency deviation at the gauge concerned.

These frequency deviations were reported in every gauge for every breaking wave, in every experiment. The smallest frequency deviation in the gauges array for each breaking wave was then noted as the level to detect, and this information gave an insight on the threshold to use for the detection. This entire information can be found in appendix A (the first three experiments were not tested). The boxes noted x mean that the wave elevation at this gauge was under 1.5 of the standard deviation or that the frequency deviation was very small. The results show that an easy and efficient threshold for the deviation of the frequency for breaking waves is around 3 radians/s. In fact, the peak frequency for these experiments is ranged between 3.14 radians/s and 3.9 radians/s. The frequency deviation is a little bit higher for the experiments that have a higher peak frequency, but we found that the lowest breaking wave frequency deviations are always around 3 radians/s. Therefore, the detection level can be adjusted by 0.1 or 0.2 radians/s

(in our case to 2.8 for the experiments with $F_p = 3.14$ radians/s and 3.1 or 3.2 for the ones with $F_p = 3.9$ radians/s) around 3 to obtain a satisfactory detection level. This means an overall ratio $\frac{F.dev}{F_p} = 0.80$ to 0.85 depending on the amount of false detection allowed.

This threshold was used in different experiments and showed very good results (see Appendix D). It is very efficient in the real breaking wave detection since we can expect from 95% to 100% detection of real breaking waves. On the other side, the false detection is limited to about 10 %, which means that for an experiment containing 100 breaking waves, we can expect the detection of 110 breaking waves, 100 of which are breaking and about 10 false breaking events. This is very encouraging and we will see in the next paragraph other parameters which can be implemented in order to decrease the amount of false breaking detection. Of course, the increase of the two parameters employed above (i.e. the wave height and the frequency deviation) will decrease rapidly the amount of false detection, but will also decrease the real detection percentage. Therefore, the parameter can be adjusted so that no false detection is allowed. Figure 19 shows an example of the detection model using the two parameters on experiment 5. The only waves that are detected are the ones that are really breaking.

Other parameters have been studied in order to increase the skills of this detection model. Most of them are simple parameters and prove to be more or less efficient in the goal of dismissing the false breaking. No parameter was found that can dismiss all the

false detection, since many of these waves that are not breaking but are detected have very close characteristics with the real breaking waves. It is therefore impossible to identify all of them.

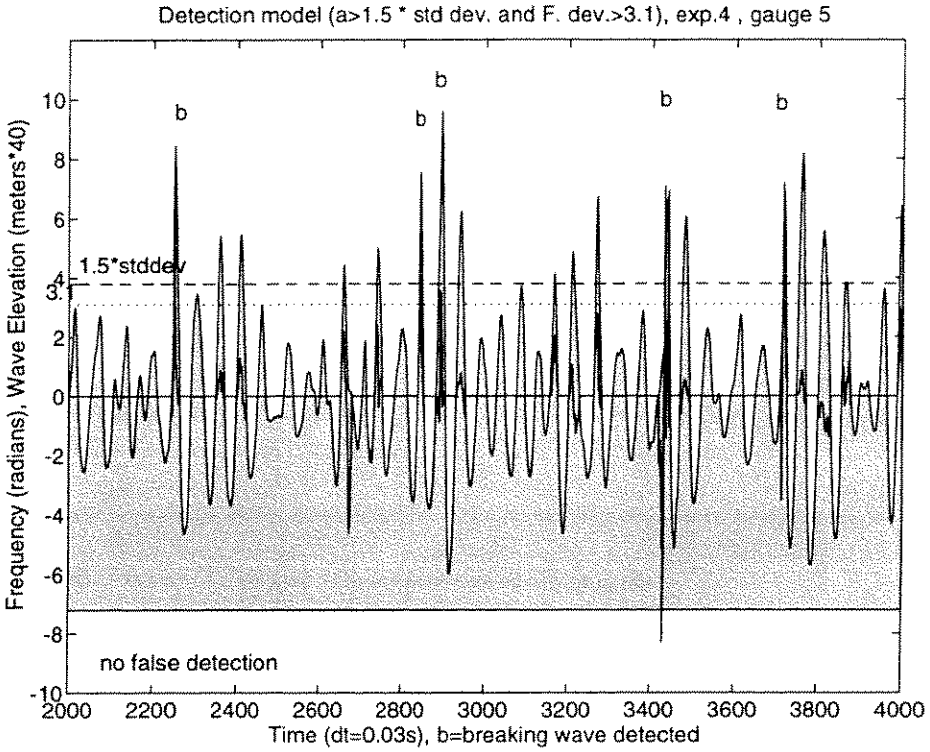

Figure 19. Breaking wave detection model.

One of the main parameters that was studied is the Hilbert Amplitude. The Hilbert Amplitude is defined as the signal:

$$A(t) = [u^2(t) + v^2(t)]^{\frac{1}{2}} \tag{45}$$

which is the amplitude of the analytic signal $\psi(t)$ described in chapter III.

This Hilbert amplitude looks like an envelope of the elevation data, as you can see in Figure 20. It shows some characteristics like a clear asymmetry between the front and rear of the wave, but is very similar in every wave detected by the model, real or false. *Griffith et. al* [1996] studied this parameter and found that the asymmetry of the Hilbert Amplitude is more pronounced for the steeper waves, but our experiments do not show any big difference between the big breakers and the non breaking waves in the asymmetry. We studied the steepness and slope of the Hilbert Amplitude in the front face of waves. We implemented these parameters in the detection model, and if it shows some ability to reduce greatly the false detection, it also reduces the detection of many real breaking waves. Indeed several breaking waves did not show a very steep Hilbert Amplitude.

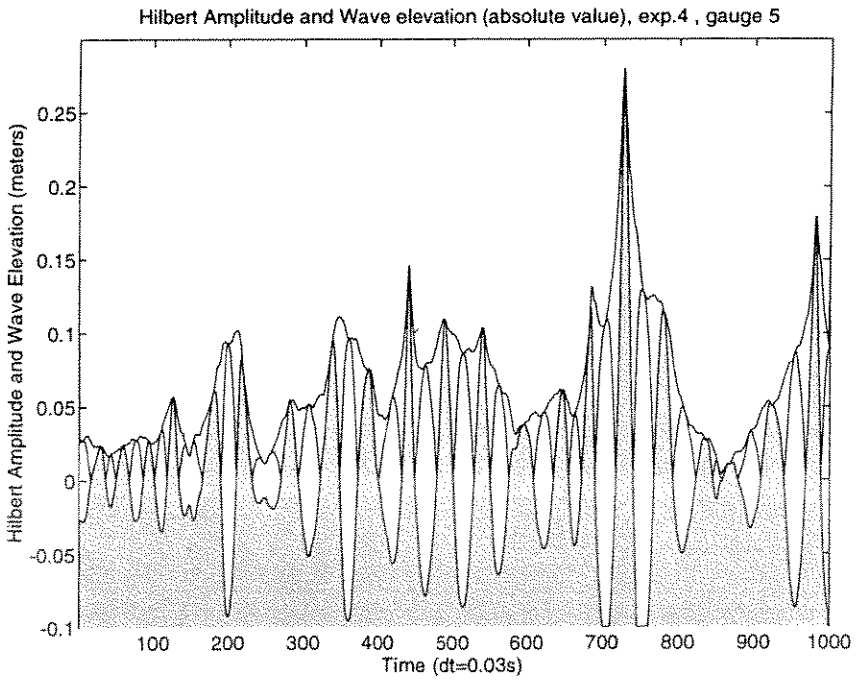

Figure 20. Hilbert amplitude and wave elevation.

We also studied different parameters such as the frequency signal slope, and different wave elevation parameters such as the crest front steepness, the horizontal asymmetry, the vertical asymmetry and others, but these do not show a great improvement in the skill in the discrimination of the false detection since the false breaking waves are very close in geometry to the real breaking waves. Since the Phase-Time Method and its Hilbert frequency is very close and related to the elevation change rate and the Hilbert transform rate of change, most of these parameters do not add much information to the Hilbert frequency. Moreover, since breaking of waves in the ocean occurs when a multitude of high frequency components build on top of a large low frequency wave, the asymmetry parameters of the elevation record would be useless, since a wave could be very asymmetric and still not have sufficient energy to break.

Sampling reduction

One of the objective at the beginning of this research was to determine how slowly the data record could be sampled without losing the ability to detect the breaking using the model.

The original sampling rate was 33 Hz and proved to be very effective when the model was used. Since the periods of our experiments are ranged between 1.6 sec. and 2 sec., and since the real ocean waves can have a period as long as 10 to 20 seconds, the model should be used with a sampling rate of about 3 Hz in the ocean to obtain the same accuracy (ratio on the order of 10).

A sampling rate this high is not typically used in the ocean. Sampling is common at 1 Hz or exceptionally at 2 Hz. Therefore we needed to examine the possibility of reducing the sampling rate without losing the ability of detecting the breaking waves. This was done by decimating the time-series coming from the original data set. The time-series were sub-sampled at 16 Hz and 8 Hz and the Phase-Time Method was applied to these "new" time-series. The results are not very satisfying. If the 16 Hz sub-sampled signal shows some ability in the detection of the breaking waves, the frequency deviation signal is very altered in the 8 Hz sub-sampled signal and is completely useless for the detection of the breaking waves. An example of the effects of the different sampling rates on the frequency deviation signal is shown Figure 21.

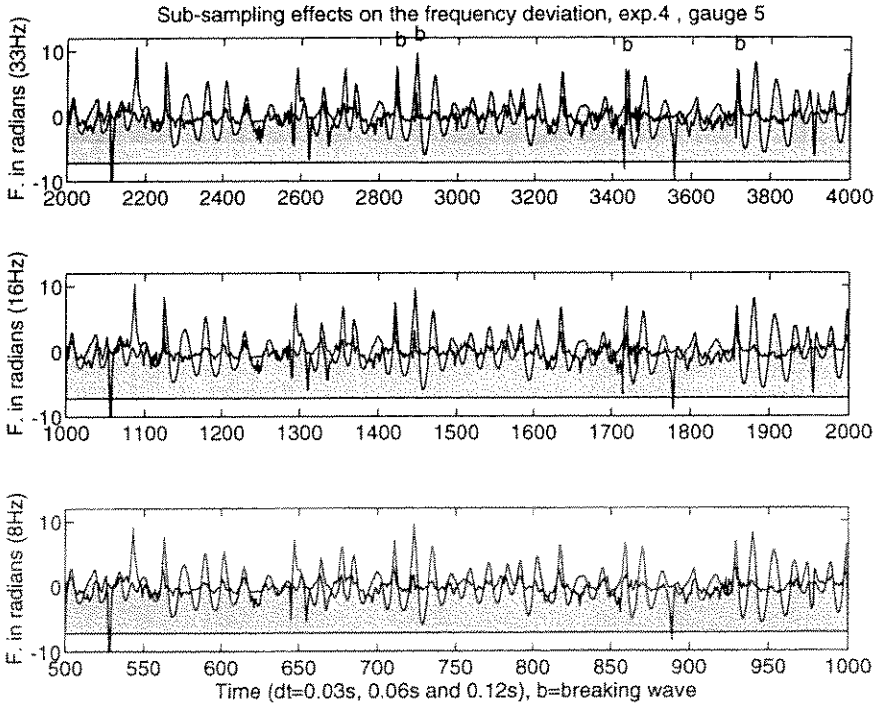

Figure 21. Sub-sampling effects on the local frequency deviation.

These results show that the model can be tried at a sampling rate of 1.5-2 Hz in the real ocean and might show some good accuracy, but this accuracy would greatly improve if the technology used would allow a faster sampling rate.

CHAPTER V

SUMMARY AND CONCLUSIONS

This research effort focused on exploring the feasibility of the Phase-Time Method as a detection method for deep water breaking waves. Application of this study includes the development of a detection model, based on a few parameters. The mathematical aspects of this research focused on the study of the Hilbert transform and Phase-Time Method and their physical meaning. The experimental investigation was directed toward obtaining a quality data set under a variety of deep water wave conditions with a substantial number of breaking waves and a video documentation to witness the breaking events. The data analysis focused on the study of the local frequency deviation obtained from the Phase-Time Method and its characteristics, toward the appreciation of its ability to identify the breaking waves from the non-breaking waves based on the wave elevation record.

The basic Hilbert transform which was utilized and studied in this research was investigated and formulated by different authors in the past like *Melville* [1982], *Hwang et al.* [1989] and *Huang et al.* [1992]. The Phase-Time Method that is studied and explored in the research was described by *Huang et al.* [1992] who studied the local properties of the ocean surface waves by applying this analytical method to their data.

This method uses a wave elevation time-series and the Hilbert transform to obtain a time-series of the local frequency deviation. *Huang et. al* placed a special attention on the eventual use of this Method as a detection tool for breaking waves.

A total of 12 experiments were conducted in the Offshore Technology Research Center basin to obtain a quality data set. These experiments had a wide range of heights and periods in order to cover a large variety of deep water waves. The duration of the experiments was 16 minutes, with a sampling rate of 33 Hz, using an 11 gauges linear array to measure the wave elevation. Part of these experiments were used in the data analysis and the development of a simple detection model and the rest were set aside to validate the model.

The investigations of the formulations of the Hilbert transform and Phase-Time Method were done in the attempt of understanding the physics of this method and determining the possibilities or limits of this method when used on a wave elevation time-series data set.

The data analysis was done by applying the Phase-Time Method on the data set, and by using the video documentation aside to visually confirm whether or not the breaking events did occur. Observation of high values of local frequency deviation associated with breaking waves were noted and led to the characterization of patterns in the local frequency signal during the breaking events. Averaged local frequency deviation patterns

were defined for incipient breaking waves, and a double peak deviation was also defined for large breaking waves.

A simple detection method was developed, using the wave Height as a first parameter to filter certain large frequency deviations which are not related to breaking and make it useful in detecting breaking events. The second parameter is the local frequency deviation signal which was clearly higher in case of breaking waves. A threshold based on the spectral peak frequency was defined, and the limits of this simple detection model were stated.

Other parameters were studied, some of which, like the Hilbert Amplitude show some potential in improving the accuracy of the model, but none of these parameters show an indisputable efficiency and somewhat reduce the amount of real breaking events detected.

This research showed first of all that the Phase-Time Method is clearly efficient in the detection of breaking events in a wave elevation time-series. It is also clear, when we looked at the physics of the method, that it can not have an efficiency of 100 %. The breaking process in the ocean is a very complicated process, and this makes the development of a detection model based on this method and accurate at 100 % almost impossible. The model we developed showed some very high real breaking detection skills (95% at least) and a pretty low false breaking detection level (less than 10 %). We

also found some characteristic patterns in the local frequency of the breaking waves which are very useful in the eventual use of this method to real ocean waves.

In conclusion, I would say that the complexity of the breaking phenomenon in the oceans makes the development of a 100% accurate detection model unlikely. But since the goal of the breaking detection is more of a statistics or probabilistic view, the use of a simple model based on the Phase-Time Method which uses only Wave Elevation data can reveal very satisfactory results.

REFERENCES

Banner, M.L., and D.H. Peregrine, Wave breaking in deep water, *Annu. Rev. Fluid Mech., 25,* 373-397, 1993.

Griffin, O.M, R.D. Peltzer, H.T. Wang, and W.W Schultz, Kinematic and dynamic evolution of deep water breaking waves, *J. Geophys. Res., 101* (C7), *16,* 515-16, 531, 1996.

Holthuijsen, L.H., T.H.C. Herbers, Statistics of wave breaking observed as whitecaps in the open sea, *J.Phys. Oceanography, 16,* 290-97, 1986.

Huang, N.E., S.R. Long, C.C. Tung, M.A Donelan, Y. Yuan, and R.J. Lai, The local properties of ocean waves by the phase-time method, *J. Geophys. Res. Lett., 19(7),* 685-688, 1992.

Hwang, P.A., D. Xu, J. Wu, Breaking of wind generated waves: measurements and characteristics, *J.Fluid Mech., 202,* 177-200, 1989.

Keller, W.C., W.J. Plant, G.R. Valenzuela, Observation of breaking ocean waves with coherent microwave radar, in *Wave Dynamics and Radio Probing of the Sea Surface*, edited by O.M. Phillips and K. Hasselmann, pp. 295-313, Plenum, New York, 1986.

Long, S.R., The Hilbert spectrum, A new tool for non-steady time series analysis, *Proceedings of the Symposium on the Air-Sea Interface*, edited by M. Donelan, Kluwer Acad., Norwell, Mass., 1996.

Longuet-Higgins, M.S., On wave breaking and the equilibrium spectrum of wind-generated waves, *Proceedings R. Soc. London Ser., 310*, 151-159, 1969

Longuet-Higgins, M.S., N.D. Smith, Measurements of breaking by a surface jump meter, *J. Geophys.Res., 88*, 9823-9831, 1983.

Melville, W.K., The instability and breaking of deep-water waves, *J. Fluid Mech., 115*, 165-185, 1982.

Poularikas, A.D., S.L. Hahn, The transforms and applications handbook, Boca Raton, Fla., CRS Press, 1996.

Snyder, R.L., R.M. Kennedy, On the formation of whitecaps by a threshold mechanism, part 1: basic formation, *J. Phys. Oceanogr., 13*, 1482-1492, 1983.

Thorpe, S.A., P.N. Humphries, Bubbles and breaking waves, Nature, *283*, 463-465, 1980.

APPENDIX A
Breaking Waves
Experiment 1

GAUGE	1	2	3	4	5	6	7	8	9	GAUGE	1	2	3	4	5	6	7	8	9	GAUGE	1	2	3	4	5	6	7	8	9
TIME										TIME										TIME									
21'15				I	I					28'42	I																		
21'16								I	S	29'17	I	S	S																
21'41	I	S	S							29'18		I	S	S	S			S											
21'42						I	S		I	29'45						I													
21'55			I	S	M					30'15	I	I	S	M	M														
21'57								I	S	30'49	I																		
22'21	I									31'06				I	I														
22'23					I					31'10	I	S	M	L	M														
22'38						I	I		I	31'17	I	I																	
22'43			I	S	M					31'24	I	S																	
23'01		I	I							31'27				I	S	S	I												
23'35			I	M	S					31'46	M	S																	
23'47	M									31'55	I	S	S																
23'48				I	S	S				31'58	S	S																	
23'59	M	S	S							31'59					I	S	S												
24'01						I	S			32'08	S																		
24'03					I	S	M			32'11							I	S	M										
24'19	I									32'39					I	S	M												
24'26	I									32'45	M																		
24'28	M	L	L	L	M					32'47						I	M	M	S										
24'45	I									32'57		I																	
24'57				I	S					33'01					I	I	S	L	L										
24'59							I	S	M	33'39	I	I	I	I	S														
25'10	I									33'42							I	S	I										
25'18			I	S						33'57					I	I													
25'39	S	S								33'58	I	I	S	S															
25'41				I	S	L	L	L	S	34'18	I	I	S	S															
26'15	S									34'28	S	S	S																
26'16				I	S	S	S	S	S	34'40	I	S																	
26'31	I	I	S	M	M					34'45	I	S																	
26'40									I	35'00						I	S	S											
26'44						I	I			35'16								I	M										
26'58		I								35'30									I										
27'02				I	S	S				35'40		I	S	I															
27'08		I	I	S						35'50				I	S	M	S												
27'11									S	36'00	I	S																	
27'16						I	S			36'17	L																		
27'40	S	S	S							36'40	M																		
27'42						I	S	M	L	36'42								I	I										
27'51	S	S								37'03	I	S	S	S	S														
28'05	I									37'10			I	S	M	S													
28'07			I	S	S					37'44	S																		
28'15			I	S	S					37'46				I	M														

I: incipient S: small M: medium L:large Peak of breaking

Breaking Waves
Experiment 2

GAUGE	1	2	3	4	5	6	7	8	9
TIME									
37'34	S								
37'36							I	S	L
37'58	I	I							
38'02							I		
38'14	I	M	M						
38'17								I	S
38'23				I	I				
39'09	S	M	S	S					
39'11							I	S	S
39'21						I			
39'30	I	S	M	M					
39'33									S
39'36			I	S	S				
39'41	S	M	S	S					
40'06					I	S	S		
40'19							I	I	
40'41	S								
40'43					I	S			
40'57			I	I					
41'00		I	S						
41'08	I	S							
41'14				I	S	M	L	L	M
41'25				I	S	M			
41'33	S	I							
41'40							S	M	M
41'56			I						
42'02	M								
42'04						I	S	S	
42'24				I	S	S			
42'28	I								
42'30	L	L	L	M					
43'03	M	S							
43'05							I	S	S
43'07	I	S	S						
43'14					I	S	S		
43'18		I	I						
43'29	S	I							
43'39	S								
43'41					I	M	L	M	
44'02		I	S						
44'06	S	S	M	L					
44'16							I	S	
44'28			I	I					

GAUGE	1	2	3	4	5	6	7	8	9
TIME									
44'32					I	S	S	I	
44'35	M								
44'38							I	S	S
44'52						I	S	S	
45'05				I	I	S	M	S	
45'15	S								
45'17					I	S			
45'24	I	S	M	S	S				
45'26			I	I					
45'55		I	M	L	M	S	S	S	S
46'36					I	I	I		
46'42		I	M	L	L	L	M	M	S
47'06	I	M	L	L	L	S			
47'15		I	S	S					
47'17	M	L	L	L	M				
47'24					I	I	S	M	L
48'10	I	S	S						
48'27			I	I			I	I	
48'32	S	S	S	M	S				
48'35	M	M	S						
48'52				I	I				
49'00			I	S	S				
49'06	I	S	M	M					
49'19		I	S	I					
49'25					I	I	M	L	L
49'48							I		
50'00		I	M	M	M				
50'11		I	S	M	M	S			
50'19	I	S	S						
50'46			I	I	S				
50'51			I	I	S	S			
51'04		I	S	S					
51'26			I	S	M	S			
51'39	L	M							
51'51						I	S	S	
51'52	I	S	M	M	M	S	S		
52'02	L	M							
52'46	M	M	M	S	S				
53'13	I	S	M	M	M	S			
53'33	S	S	S	S					
54'05	S	S							
54'07								M	
54'29	I	S	S						

GAUGE	1	2	3	4	5	6	7	8	9
TIME									

I: incipient S: small M: medium L:large

Peak of breaking

Breaking Waves
Experiment 3

GAUGE	1	2	3	4	5	6	7	8	9
TIME									
17'14		I	S	S	S	S	S		
17'30					I	M	S		
17'37				I	I	S			
17'51		I	S	L	L	M	M	S	M
18'56	S								
19'01						I	I		
19'09	M	L	S	S					
19'25				I	S				
20'03	I	S	S						
20'11		I	S	S					
20'21				I	S	S			
20'48	S								
21'20		I	I						
21'24	I	S							
21'50	I	S	S						
22'02	S								
22'04					I	I			
22'18	I	S	S						
22'20					I	S	S		
22'26				I			I	I	
22'34			I	S					
22'51	I	S	S	I					
23'10	M	M	L	M	M	S			
23'48		I	I						
23'57	L	M	S	S					
24'09					I	S	S		
24'24		I							
24'40			I	S	M	M	M	M	
25'01				I	S	L	L		
25'37	I	S	S	M	M				
26'06				I	I	S	S		
26'15	I	S	S						
26'34	I	S	M	L	M	M	S	S	
27'05					I	I			
27'09				I	S	S			
27'29			I	I					
27'42					I	S	M	M	S
27'59		I	S	S					
28'15							I	S	S
28'22					I	S			
28'38		I	S	S					
28'45			I	S					
29'22	I								

GAUGE	1	2	3	4	5	6	7	8	9
TIME									
29'25							I	M	M
29'49						I	S		
30'20						I	I	I	
30'41	I								
31'08	M								
31'10					I	S	S		
31'17					I	S	S		
31'34	S								
31'37	S								
31'58	S	S							
32'24	S	S							
32'50			I	I					
32'57				I					
33'09					I	S			
33'23				I	S				
33'33				I	S	M			
33'34	I	S	S	S					
33'45			I	S	I	I	I	I	

GAUGE	1	2	3	4	5	6	7	8	9
TIME									

I: incipient S: small M: medium L: large

Peak of breaking

Breaking Waves
Experiment 4

GAUGE		1	2	3	4	5	6	7	8	9	10	11	1	2	3	4	5	6	7	8	9	10	11	F. dev.
TIME	DATA																							(rad)
0:55	150	I	S	S									9.2	7.6	4.5									4.5
1:03	417					I	I										5.0	3.7						3.7
1:12	717			I	M	L	M								3.6	3.2	3.3	4.9						3.2
1:19	950			I	S	S									4.4	3.5	3.1							3.1
1:27	1217		I	S	M									8.7	9.0	13								8.7
1:30	1317									I	S	M									7.6	8.4	7.1	7.1
1:56	2184	I	I	S									4.6	6.6	x									4.6
1:58	2250					I	S	M									7.3	8.5	6.2					6.2
2:14	2784	S											4.9											4.9
2:16	2850					I	S	M	S								5.6	7.5	6.2	3.8				3.8
2:16	2850	I	S	S	S	S							5.7	4.3	4.1	3.6	3.5							3.5
2:28	3250						I	S										3.0	x					3
2:33	3417		I	S	L	M								7.3	8.7	4.5	7.0							4.5
2:41	3684				S	M	M									7.9	7.1	8.7						7.1
3:00	4317						I	S	M	M	S							7.2	5.2	7.1	5.0	3.5		3.5
3:13	4750	S	I										7.5	10										7.5
3:15	4817							S											7.3					7.3
3:35	5484						I											4.3						4.3
3:40	5650				I											x								x
3:41	5684							I											8.7					8.7
3:53	6084		I											6.0										6
3:54	6117								I	S										6.7	4.9			4.9
4:05	6484				I	M	M	S								5.2	6.2	3.5	3.0					3
4:22	7050	S											3.8											3.8
4:26	7184		I	S	S	M	M	S						5.2	8.1	7.4	5.9	5.8	5.3					5.2
4:35	7484			I	S	S									7.9	4.9	4.2							4.2
4:38	7584			I	M	S									7.4	5.3	3.5							3.5
4:54	8117	I	S	S									6.9	6.5	5.3									5.3
4:57	8217		I	S										8.9	6.0									6
5:08	8584		I	I										3.1	4.7									3.1
5:40	9650					I	I										7.0	x						7
5:42	9717									I	I	I									4.6	5.6	3.5	3.5
5:56	10184	M											5.9											5.9
5:58	10250						I	I										4.7	5.2					4.7
6:31	11350		I	I	I									9.2	7.0	x								7
6:35	11484										I	I										9.2	10	9.2
6:44	11784	M											4.2											4.2
6:51	12017				I	S	S									6.0	4.4	3.4						3.4
6:59	12284		I	S										7.5	4.1									4.1
7:07	12550				I	M	M									10	6.0	11						6
7:22	13050	M											8.6											8.6
7:25	13150							I	S	S									4.1	4.4	4.7			4.1
7:42	13717			I	S	S	S								x	x	x	x						x
I: incipient S: small M: medium L:large																		Peak of breaking						

Breaking Waves
Experiment 4

GAUGE		1	2	3	4	5	6	7	8	9	10	11	1	2	3	4	5	6	7	8	9	10	11	F. dev.
TIME	DATA																							(rad)
7:54	14117				I	S	S	S								5.4	6.6	7.1	5.8	4.4				4.4
8:01	14350	I	S	S									7.6	4.7	5.2									4.7
8:12	14717							I	I										7.7	6.4				6.4
8:35	15484	I	S	I									7.5	6.4	x									6.4
8:57	16217	I	I	S	S	S							3.1	5.3	x	5.6	3.6							3.1
9:07	16550	I	S										3.6	x										3.6
9:09	16617								I	S	M	S								6.9	4.3	9.3	3.5	3.5
9:14	16784		I	S										6.2	5.0									5
9:24	17117						I	I	S	M	L	M						4.0	6.7	9.8	10	8.8	7.4	4
9:41	17684			I	S	I	I								5.6	3.0	4.0	4.6						3
10:09	18617				I	S	S									7.5	5.3	4.2						4.2
10:18	18917								I	S	S									5.8	3.9	3.8		3.8
10:21	19017				I	S	S	S	S	S	S					5.1	5.4	3.5	5.7	4.9	5.0	3.8		3.5
10:30	19317				I	M	S									4.6	3.1	x						3.1
10:46	19850					I	S										5.7	7.5						5.7
10:59	20284				I	S	M									6.1	6.3	5.3						5.3
11:22	21050			I	S	S	M	L	S						3.1	4.6	6.7	7.1	6.9	x				3.1
11:33	21417							I	I										5.0	7.4				5
11:50	21984							I	I										x	3.3				3.3
11:56	22184					I	S	M									6.3	6.9	4.9					4.9
12:01	22350	M											5.1											5.1
12:30	23317	I	S	S	M	S							3.0	7.4	8.2	3.9	5.2							3
12:45	23817				I	S	I									4.9	4.2	4.1						4.1
12:49	23950	I	S	S									x	4.0	x									4
12:58	24250							I	S										6.1	5.1				5.1
13:30	25317		I	S	S									5.1	8.1	4.1								4.1
13:34	25450				I	I	S	M	M							x	6.6	7.2	7.5	5.0				5
13:56	26184	S	S										8.4	5.6										5.6
13:58	26250						I	S	S									5.3	4.6	6.4				4.6
14:08	26584	I	I	S									5.4	6.7	4.8									4.8
14:51	28017					I	S	S									6.3	6.9	x					6.3
14:55	28150					I	I										6.4	4.8						4.8
15:22	29050					I	S	S									7.2	7.0	8.5					7
15:32	29384			I	S	M	S								5.8	7.3	4.3	4.2						4.2
15:41	29684				I	S	S	I								x	4.6	4.3	x					4.3
15:43	29750		I	I	S	S								6.8	6.0	5.6	4.4							4.4
16:25	31150		I											x										x
17:05	32484			I	I										4.6	3.8								3.8
17:26	33184		I	S										x	x									x

I: incipient S: small M: medium L:large | Peak of breaking

Breaking Waves
Experiment 4-2

GAUGE		1	2	3	4	5	6	7	8	9	10	11	1	2	3	4	5	6	7	8	9	10	11	F. dev
TIME	DATA																							(rad)
16:39.0	150	I	S										8.9	4.9										4.9
16:56.0	726			I	S	S	S								4.0	x	4.2	4.5						4
17:03.0	960				I	I										x	3.9							3.9
17:11.0	1226		I	S	S									8.0	9.0	7.9								7.9
17:41.0	2226					I	S	S									7.7	4.8	4.2					4.2
17:59.0	2826					I	S	S									6.7	8.3	7.0					6.7
18:00.0	2860	I	S	S	S	S							5.6	3.5	4.7	4.0	3.2							3.2
18:17.0	3426		I	S	S									9.2	8.2	8.0								8
18:25.0	3693			I	S	S									6.6	10	5.9							5.9
18:44.0	4326					I	S	S	S								5.4	7.5	5.7	4.9				4.9
18:59.0	4826						I	S										6.7	5.0					5
19:49.0	6493			I	S	S									5.1	3.8	4.9							3.8
20:10.0	7193			I	S	M	S								7.6	8.4	7.3	5.3						5.3
20:19.0	7493			I	S	S									8.0	x	4.7							4.7
20:22.0	7593			I	S	S									6.5	6.4	3.4							3.4
20:41.0	8226			I	S	S									9.0	8.0	8.8							8
21:42.0	10260							I	I										4.3	6.4				4.3
22:28.0	11793	S											x											x
22:35.0	12026			I	S	S									4.9	5.0	4.5							4.9
22:43.0	12293		I	I										7.2	6.0									6
23:05.0	13026			I	I	S									7.1	4.0	4.2							4
23:09.0	13160							I	I										5.2	6.0				5.2
23:30.0	13860			I	S	S									4.0	5.8	3.4							3.4
23:38.0	14126				I	S	S									10	9.6	8.8						8.8
23:45.0	14360	I	S										4.6	4.5										4.5
24:14.0	15326	I	S	S									x	x	x									x
24:41.0	16226	I	I	S	S	S	S						x	6.7	4.1	4.9	3.3	7.2						3.3
24:52.0	16593							I	S	S									6.2	7.4	5.7			5.7
24:58.0	16793	I	S	S									5.9	4.8	5.0									4.8
25:08.0	17126							I	S	S	M								8.3	9.0	16	9.4		8.3
25:53.0	18626				I	S	S									7.1	3.9	4.0						3.9
26:02.0	18926							I	S	M									5.0	6.5	x			5
26:05.0	19026				I	S	S	S								4.7	4.0	x	5.9					4
26:21.0	19560		I	S	S									4.2	10	8.1								4.2
26:43.0	20293			I	S	S	S	S							4.6	5.8	4.6	4.0	6.3					4
26:59.0	20826			I	S	S									3.4	5.7	4.7							3.4
27:05.0	21026			I	S	S	M	M							3.5	4.6	10	5.0	9.9					4.6
27:40.0	22193				I	S	S	S								4.1	6.3	5.3	x					4.1
28:13.0	23293	I	S	S	S								4.8	8.7	5.8	x								4.8
28:29.0	23826		I	I	I									4.2	4.5	4.7								4.2
28:39.0	24160	S	S	S									7.8	7.6	7.2									7.2
29:01.0	24893		I	S										3.2	x									3.2
29:17.0	25426				I	S	M	S								7.4	5.6	5.7	4.9					4.9
I: incipient S: small M: medium L:large																	Peak of breaking							

Breaking Waves
Experiment 4-2

GAUGE		1	2	3	4	5	6	7	8	9	10	11	1	2	3	4	5	6	7	8	9	10	11	F. dev.
TIME	DATA																							(rad)
29:40.0	26193	S	S										6.4	3.3										3.3
29:42.0	26260					I	I	I	I								3.9	3.8	6.7	4.6				3.8
30:34.0	27993				I	S										3.6	5.9							3.6
31:05.0	29026				I	I	S									3.7	7.3	4.8						3.7
31:16.0	29393		I	S	S									6.1	8.4	3.7								3.7
31:24.0	29660				I	S	S									4.4	5.4	3.7						3.7
31:27.0	29760		I	S	S									6.3	6.6	4.9								4.9
32:48.0	32460			I	I										6.7	4.3								4.3
32:52.0	32593				I	S	S									4.4	4.4	x						4.4
32:54.0	32660									I	S	M									6.1	5.0	x	5

I: Incipient S: small M: medium L:large | Peak of breaking

Breaking Waves
Experiment 5

GAUGE		1	2	3	4	5	6	7	8	9	10	11	1	2	3	4	5	6	7	8	9	10	11	F. dev.
TIME	DATA																							(rad)
48:59.0	1249							I	S	S									5.7	5.7	4.4			4.4
49:07.0	1516								I	S										3.9	3.2			3.2
49:10.0	1616	I	I	S	S	I	S	M	S				x	x	x	3.0	5.0	5.8	4.3	x				3
49:25.0	2116			I	I	S	S								3.7	3.9	3.5	3.9						3.5
49:53.0	3049		I	I	S	S								5.9	4.4	6.3	x							4.4
49:55.0	3116								I	S	L	L								8.8	6.4	4.4	3.5	3.5
49:55.0	3116			I	M	L	L	M	S						6.5	5.7	5.7	4.4	3.3	5.4				3.3
50:08.0	3549			I	I	S	M	S							5.9	8.2	8.7	5.1	4.6					4.6
50:19.0	3916			I	S	M	M	S							4.2	6.9	3.4	6.1	8.9					3.4
50:23.0	4049		I	I	S	L	M							4.8	5.1	6.0	3.2	x						3.2
50:31.0	4316				I	S	S									3.8	5.9	4.3						3.8
51:03.0	5382				I	I										3.1	6.9							3.1
51:36.0	6482	I	S										6.7	5.6										5.6
51:44.0	6749	I	S	S	I	I							4.8	4.6	4.5	3.9	3.8							3.8
51:50.0	6949							I	S	S	S								3.7	4.6	3.7	3.3		3.3
52:16.0	7816				I	I	I									x	5.9	6.6						5.9
52:20.0	7949									I	I										5.5	3.1		3.1
52:44.0	8749							I	I	I	I								6.3	5.5	6.4	4.5		4.5
52:50.0	8949	I	S	S									4.3	3.6	3.8									3.8
52:59.0	9249	M	L	L	L	L	M	S					5.5	3.5	3.1	5.1	4.3	3.9	3.7					3.1
53:19.0	9916	I	S	L	L	M							5.0	4.0	x	5.7	4.3							4
53:46.0	10816	S	S	S	S	S							5.4	4.5	4.4	6.7	4.9							4.4
53:50.0	10949				I	S										x	x							x
53:57.0	11182							I	S	S									8.2	11	10			8.2
53:58.0	11216				I	S	S	M	M	M	M	M				3.4	5.1	5.6	6.5	9.4	9.8	11	5.5	3.4
54:29.0	12249			I	S	M	M	M	M	M	M				6.3	4.3	3.7	5.7	6.5	6.6	14	8.2		3.7
54:44.0	12749		I	S										8.3	6.4									6.4
55:07.0	13516			I	I	I	I								4.4	x	4.1	x						4.1
55:28.0	14216	I	S	S									7.0	4.9	x									4.9
55:37.0	14516				I	I	S	S								4.5	7.3	5.5	3.9					3.9
55:48.0	14882							I	S	M									6.6	7.7	4.4			4.4
56:34.0	16416				I	S	S	S	S							8.7	3.7	7.6	6.6	6.3				3.7
57:33.0	18382		I	I										4.6	5.2									4.6
58:25.0	20116							I	I	S	M	M							5.3	6.6	5.1	3.8	3.0	3
58:33.0	20382							I	S	S	S								7.1	5.8	8.2	5.9		5.8
59:01.0	21316				I	I	I	I	S							4.2	3.0	6.3	4.7	3.2				3.2
59:12.0	21682	I	S	S	S								6.0	7.5	4.6	4.2								4.2
59:28.0	22216					I	S	S	S								5.8	5.2	3.7	4.7				3.7
00:01.0	23316		I	S	S									7.1	6.0	4.2								4.2
00:08.0	23549	S											6.6											6.6
00:10.0	23616							I	S										7.8	8.6				7.8
00:17.0	23849					I	S	S	M	M	M						6.6	6.8	7.8	6.1	5.4	4.2		4.2
00:45.0	24782				I	S	S									7.5	7.4	5.6						5.6
I: incipient S: small M: medium L:large																	Peak of breaking							

Breaking Waves
Experiment 5

GAUGE		1	2	3	4	5	6	7	8	9	10	11	1	2	3	4	5	6	7	8	9	10	11	F. dev.
TIME	DATA																							(rad)
00:54.0	25082	S	S										12	6.1										6.1
00:56.0	25149							I	S										5.3	3.9				3.9
01:17.0	25849	I	I	I	S	M							3.3	8.5	6.0	3.8	6.6							3.8
01:24.0	26082	S											7.7											7.7
01:27.0	26182								I	I	S	S								5.5	7.4	6.2	5.5	5.5
02:04.0	27416					I	S	S									6.0	3.8	3.6					3.6
02:16.0	27816								I	I	I									4.6	5.9	7.9		4.6
02:29.0	28249		I	S	S	S								6.7	5.0	5.2	4.1							4.1
02:34.0	28416	S	S	S									3.7	x	3.3									3.3
03:11.0	29649			I	S	S									3.9	3.2	x							3.2
03:36.0	30482	I	S	S									5.1	5.4	5.0									5
03:45.0	30782			I	S	S									3.8	5.7	3.9							3.8
03:58.0	31216							I	S	S									7.3	5.3	8.0			5.3
04:10.0	31616		I	S	S	S								6.0	7.1	7.1	3.5							3.5
04:39.0	32582							I	S	M	M								8.2	7.4	5.1	6.1		5.1

I: incipient S: small M: medium L:large

Peak of breaking

Breaking Waves
Experiment 6

GAUGE		1	2	3	4	5	6	7	8	9	10	11	1	2	3	4	5	6	7	8	9	10	11	F. dev.
TIME	DATA																							(rad)
40:31.0	960							I	I	S									3.7	4.5	3.4			3.4
40:36.0	1127	S	S	S									5.9	6.1	3.5									3.5
41:01.0	1960								I	S	M									3.6	12	x		3.6
41:28.0	2860							I	I	S	S	S							3.5	3.7	5.5	3.8	6.1	3.5
41:38.0	3194								I	I	S	S								7.3	4.7	9.8	11	4.7
41:48.0	3527							I	S										3.0	5.0				3
42:04.0	4060				I	S	S									6.5	7.4	x						6.5
42:28.0	4860					I	I										3.9	3.2						3.2
42:37.0	5160			I	S	S									x	x	x							x
42:56.0	5794				I	S	S	S								4.8	3.0	5.3	3.9					3
43:22.0	6660					I	I	I	I								5.3	5.4	5.9	3.6				3.6
43:26.0	6794	S	S										4.1	x										4.1
43:33.0	7027	S	S	M	S	S	S	S					5.2	5.3	3.3	3.6	3.9	2.8	6.4					2.8
44:00.0	7927	I	S	I	S								3.9	4.9	4.6	2.8								2.8
44:12.0	8327		I	I	S									4.2	5.5	3.4								3.4
44:22.0	8660					I	I	I	I								3.5	4.4	3.2	2.8				2.8
44:49.0	9560	S	S										5.2	3.8										3.8
44:51.0	9627								I	I										5.1	3.6			3.6
45:07.0	10160		I	I	I									4.5	3.6	x								3.6
45:42.0	11327			I	I	S									4.1	4.8	3.5							3.5
45:52.0	11660	S	L	S	S	M							6.8	5.4	3.3	x	x							3.3
46:09.0	12227								I	I	I									4.2	2.9	4.0		2.9
46:17.0	12494						I	S										5.9	x					5.9
46:23.0	12694		I	S	M	S								x	5.7	4.7	x							4.7
46:56.0	13794				I	I	S									5.5	6.3	5.6						5.5
47:17.0	14494	S	M	M	S								5.9	5.5	5.3	5.1								5.1
47:30.0	14927	S	S										4.1	3.0										3
47:40.0	15260	I	S	S									2.9	6.5	6.2									2.9
47:42.0	15327	I	I	S	S								x	4.7	4.1	3.3								3.3
47:46.0	15460			I											5.9									5.9
47:56.0	15794	M	M	M	S								4.8	x	7.2	7.7								4.8
48:06.0	16127	I	S	S									5.7	5.4	5.0									5
48:08.0	16194							I	S	S									6.4	5.8	5.8			5.8
48:15.0	16427	I	S	S									9.4	10	8.4									8.4
48:33.0	17027			I	S	M									6.2	5.6	4.0							4
48:39.0	17227			I	S	M	M	M	M	S					5.3	3.0	5.5	5.0	6.8	x	6.5			3
49:10.0	18260	I	S	S									8.2	6.8	8.9									6.8
49:23.0	18694			I	S	S	S	I	S						4.7	4.1	4.2	3.3	4.0	x				3.3
49:34.0	19060			I	S	S	S								6.4	5.1	6.7	5.0						5
49:57.0	19827	S	S										5.5	3.3										3.3
50:02.0	19994		I	S	L	M								5.5	5.0	7.8	3.9							5
50:09.0	20227						I	S										6.5	5.6					3.9
51:01.0	21960							I	I	I	I								4.2	4.1	6.1	3.6		3.6

I: incipient S: small M: medium L:large Peak of breaking

Breaking Waves
Experiment 6

GAUGE		1	2	3	4	5	6	7	8	9	10	11	1	2	3	4	5	6	7	8	9	10	11	F. dev.
TIME	DATA																							(rad)
51:45.0	23427			I	I										5.1	4.3								4.3
51:50.0	23594	M	S										6.2	4.6										4.6
52:20.0	24594			I	S	S									4.2	4.5	2.8							2.8
52:21.0	24627		I	S										4.9	4.7									4.7
52:38.0	25194						I	I	I									7.7	7.1	6.0				6
52:45.0	25427	M											3.4											3.4
53:05.0	26093	I	S										4.3	x										4.3
53:47.0	27494					I	S										2.6	4.7						2.6
54:20.0	28594							I	I	S	L	M							5.5	6.2	4.3	5.7	3.0	3
54:41.0	29294	S											x											x
54:43.0	29360					I	S										5.3	8.5	11					5.3
54:53.0	29694		I	S	M	M	S							5.2	4.5	4.0	x	x						4
55:12.0	30327				I	I	S	S	S							4.5	6.0	5.7	6.2	4.3				4.3
55:23.0	30694	S	M	L	M	S							9.2	13	7.0	7.8	x							7
55:36.0	31127		I	S	M	M	M	M						3.8	5.8	4.5	7.6	3.8	x					3.8
56:01.0	31960						I	S	S									7.1	4.3	x				4.3
56:23.0	32694		I											4.5										4.5
56:26.0	32794							I	I										x	x				x

I: incipient S: small M: medium L:large

Peak of breaking

Breaking Waves
Experiment 6-2

GAUGE		1	2	3	4	5	6	7	8	9	10	11	1	2	3	4	5	6	7	8	9	10	11	F. dev.
TIME	DATA																							(rad)
45:38.0	85			I	S	S	S								4.4	5.5	3.1	3.3						3.3
46:04.0	952							I	I	S									4.7	4.4	3.3			3.3
46:09.0	1118	S	S										6.2	4.4										4.4
46:33.0	1918								I	S	M	M								16	11	x	x	11
46:51.0	2518		I	I										3.6	x									3.6
47:01.0	2852							I	I	I	S	S							3.4	4.8	6.5	3.5	2.6	2.6
47:09.0	3118			I	S	S									5.7	6.0	12							5.7
47:11.0	3185								I	I	S	S								11	11	5.8	x	5.8
47:21.0	3518							I	I										3.8	6.6				3.8
47:37.0	4052					I											5.5							5.5
48:02.0	4885							I	I										2.6	x				2.6
48:10.0	5152			I	I	S									x	x	8.2							8.2
48:29.0	5785				I	S	S	S								5.4	5.1	6.6	3.3					3.3
48:47.0	6385									I	S	S									x	10	x	10
48:54.0	6618				I	S	S	S								4.1	4.1	4.9	3.6					3.6
48:59.0	6785	I	S										x	3.2										3.2
49:06.0	7018	I	I	I	I	I	I	I					5.3	4.7	5.2	3.3	6.1	4.5	5.4					3.3
49:46.0	8352			I	I	I									5.0	4.2	4.0							4
49:54.0	8618					I	I	I									4.8	3.7	2.7					2.7
50:24.0	9618							I	I	I	I								2.7	4.7	5.0	4.6		2.7
50:40.0	10152			I	I	I									3.1	x	x							3.1
51:15.0	11318				I	S	I									4.7	6.2	4.3						4.3
51:24.0	11618	S	M	M	S								4.1	4.1	3.3	3.7								3.3
51:40.0	12152	I	I	S	S								3.2	5.4	3.5	x								3.2
51:56.0	12685	I	I	S	S								3.1	5.4	2.5	4.0								2.5
52:11.0	13185					I	I	I									5.3	5.3	4.3					4.3
52:29.0	13785			I	I	S	S	S							3.9	4.0	5.2	6.3	4.4					3.9
52:50.0	14485	S	M	M	M								7.4	6.8	5.0	3.8								3.8
53:03.0	14918	S	S	S									3.5	3.2	4.2									3.2
53:13.0	15252		I	S										6.4	7.5									6.4
53:15.0	15318	I	I	S	S	S							3.5	6.5	6.1	3.6	5.7							3.5
53:29.0	15785	S	M	M	M	S							9.1	x	4.4	6.6	2.6							2.6
53:40.0	16152		I	S										6.6	x									6.6
53:42.0	16218							I	I	I									4.7	6.6	x			4.7
53:58.0	16752	S	S										x	x										x
54:06.0	17018			I	S	M	S								4.8	5.4	5.2	4.4						4.4
54:12.0	17218			I	S	M	M	S							4.5	5.0	6.0	5.3	5.3					4.5
54:22.0	17552							I	I	S	S								3.8	4.6	3.7	5.5		3.7
54:43.0	18252	I	S										5.6	9.0										5.6
54:56.0	18685				I	S	S		S		S					4.9	3.0	3.6		5.9		3.4		3
55:07.0	19052		I	I	S	M	S	S	S					5.3	5.6	6.0	5.0	4.8	3.9	4.4				3.9
55:18.0	19418	S											2.9											2.9
55:30.0	19818	I	I	I									6.4	5.3	4.2									4.2
I: incipient S: small M: medium L:large																	Peak of breaking							

Breaking Waves
Experiment 6-2

GAUGE		1	2	3	4	5	6	7	8	9	10	11	1	2	3	4	5	6	7	8	9	10	11	F. dev.
TIME	DATA																							(rad)
55:35.0	19985	I	S	M	L	M	S						3.2	6.0	5.6	6.8	x	x						3.2
55:42.0	20218					I	I	I									6.3	10	9.2					6.3
56:34.0	21952						I	I	I	I								5.3	5.6	4.2	7.7			4.2
57:18.0	23418			I	I										6.7	3.3								3.3
57:23.0	23585	S	S										5.1	7.0										5.1
57:53.0	24585		I	I	S									4.8	4.5	3.5								3.5
57:54.0	24618	I	S										6.1	5.7										5.7
58:46.0	26352				I	I										5.7	x							5.7
59:20.0	27485				I	I	I									x	4.5	5.7						4.5
59:53.0	28585						I	I	S	M	S							3.7	6.9	5.5	7.3	3.6		3.6
59:54.0	28618	S	S										4.1	3.7										3.7
00:16.0	29352					I	I	S									5.5	8.4	16					5.5
00:26.0	29685		I	S	S	S								4.9	3.8	4.1	4.2							4.2
00:45.0	30318				I	S	S	S								5.4	6.5	3.3	x					3.3
00:55.0	30652	L	L	M									7.4	8.8	9.8									8.8
01:08.0	31085	I	I	S	M	M	S						5.3	5.5	5.6	5.5	3.8	3.7						3.7
01:22.0	31552									I	S	S									3.3	3.1	x	3.1
01:34.0	31952						I	S										6.6	6.3					6.3

I: Incipient S: small M: medium L:large

Peak of breaking

Breaking Waves
Experiment 7

GAUGE		1	2	3	4	5	6	7	8	9	10	11	1	2	3	4	5	6	7	8	9	10	11	F. dev.
TIME	DATA																							(rad)
34:22.0	120				I	S	M	M								6.4	8.2	5.6	x					5.6
34:31.0	404						I	I										4.2	3.4					3.4
34:38.0	637				I	M	L	M								5.7	6.0	3.8	3.1					3.1
34:45.0	870	I	I										5.0	x										5
34:48.0	970							I	I										7.0	x				7
35:05.0	1537	I	S	S	S	S							6.6	6.2	5.2	5.0	4.3							4.3
35:08.0	1637									I	S	S								4.2	9.5	5.5		4.2
35:24.0	2170		I	S	S	S								5.4	3.8	4.2	x							3.8
35:36.0	2570										I	M										6.4	4.7	4.7
35:39.0	2670	M	S										4.8	6.1										4.8
35:42.0	2770									I	I	S									6.8	5.7	x	5.7
35:59.0	3337	M	M	S									5.8	8.7	7.2									5.8
36:01.0	3404										I	S										5.3	3.0	3
36:10.0	3704			I	S	I									5.4	6.9	3.3							3.3
36:29.0	4337				I	M	L	S								6.4	2.9	3.8	4.6					2.9
37:26.0	6237	I	S	S									3.8	4.8	x									3.8
38:22.0	8104		I	S	S									5.3	6.4	5.3								5.3
38:24.0	8170									I	S	S									5.9	6.5	2.9	2.9
38:29.0	8337	M	S										8.0	4.3										4.3
39:11.0	9737							I	I										5.9	x				5.9
39:13.0	9804	I	I	S	S								x	9.5	x	x								9.5
39:15.0	9870								I	I	S	S								10	5.8	7.4	5.3	5.3
39:32.0	10437						I	S	S									4.3	5.4	5.6				4.3
39:52.0	11104					I	I	I	I	I	I						x	x	x	3.1	3.7	x		3.1
40:32.0	12437		I	S	S	M	S							4.0	4.6	4.7	3.7	x						3.7
41:13.0	13804						I	I	I	I	I							x	3.7	3.1	4.6	4.0		3.1
41:25.0	14204				I	I	S									4.2	4.0	4.9						4
41:55.0	15204		I	I	I									5.2	6.2	3.7								3.7
42:17.0	15937	M	M										7.0	4.5										4.5
42:18.0	15970	M											4.6											4.6
42:43.0	16804						I				S	S						6.8				x	5.7	5.7
42:50.0	17037	M	M	S	S								5.3	5.9	3.6	3.9								3.6
43:25.0	18204	S	S	S									4.2	4.8	x									4.2
43:48.0	18970	S	S										4.6	3.8										3.8
43:59.0	19337	S	S										2.8	5.1										2.8
44:09.0	19670				I	I										4.6	2.8							2.8
44:23.0	20137	S	S										4.7	3.2										3.2
44:36.0	20570	M	L										11	10										10
44:49.0	21004	I	S	M	L	M	S						6.2	6.1	x	x	3.7	x						3.7
45:00.0	21370	I	S	M	M	M	S	S					7.0	4.8	6.2	7.7	7.3	7.9	5.5					4.8
45:26.0	22237		I	S										x	x									x
45:38.0	22637	L	L										5.4	7.3										5.4
45:40.0	22704									I	I	I									3.7	x	x	3.7

I: incipient S: small M: medium L:large — Peak of breaking

Breaking Waves
Experiment 7

GAUGE		1	2	3	4	5	6	7	8	9	10	11	1	2	3	4	5	6	7	8	9	10	11	F. dev.
TIME	DATA																							(rad)
46:00.0	23370			I	S	S									4.4	6.1	7.7							4.4
46:26.0	24237		I	I		I	I	S						4.4	3.0		5.5	4.4	x					3
46:41.0	24737	I	M	M	M								7.7	7.1	7.8	8.1								7.1
46:43.0	24804	M	S										3.8	2.8										2.8
46:45.0	24870									I	S	S									5.3	5.9	3.3	3.3
46:49.0	25004	I	I	L	M	S							4.6	6.1	5.3	6.2	2.8							2.8
47:12.0	25770								I	I	I									3.9	5.3	3.1		3.1
47:21.0	26070					I	I	S	S	S							5.9	4.6	5.0	5.4	4.3			4.3
47:35.0	26537		I	S	S									4.4	3.1	6.1								3.1
47:48.0	26970			I	S	S	S								4.5	7.5	5.6	4.1						4.1
47:55.0	27204						I	I	I	S	S	I						4.5	3.8	5.9	5.0	4.3	3.1	3.1
48:11.0	27737					I	I										x	x						x
48:27.0	28270				I	S	S									5.6	4.3	3.3						3.3
48:38.0	28637	I	I										5.2	4.0										4
48:41.0	28737			I	I										4.2	3.5								3.5
48:49.0	29004	I	I	S									7.9	6.2	5.9									5.9
48:52.0	29104								I	I										6.2	5.6			5.6
48:56.0	29237			I	M	S									7.6	7.8	3.5							3.5
49:20.0	30037	S	S										4.4	2.8										2.8
49:49.0	31004	S											4.0											4
49:50.0	31037					S	I	I									4.8	4.3	3.6					3.6
50:07.0	31604						I	I	S	S								5.2	6.1	4.4	2.2			2.2
50:13.0	31804					I	S	S	S								4.4	7.8	6.2	8.9				4.4
50:28.0	32304				I	S	I									3.7	3.0	x						3
50:30.0	32370	I	I	S	S	S							3.3	6.3	4.8	3.4	4.2							3.3
50:34.0	32504			I	I	S	S								x	4.7	3.9	5.5						3.9
50:43.0	32804	S	S										o	o										
50:45.0	32870								I	I	S	S								o	o	o	o	
50:50.0	33037				I	S	S									o	o	o						

I: incipient S: small M: medium L:large Peak of breaking

Breaking Waves
Experiment 8

GAUGE		1	2	3	4	5	6	7	8	9	10	11	1	2	3	4	5	6	7	8	9	10	11	F. dev.
TIME	DATA																							(rad)
40:42.0	187	I	S	S	S								3.8	7.1	6.6	6.8								3.8
40:52.0	521						I	I	I	I								5.6	4.8	4.0	3.1			3.1
41:16.0	1321	S											5.8											5.8
41:24.0	1587	S	S	S									8.1	7.6	8.1									7.6
41:38.0	2054	I	S	M	S								6.8	7.9	3.4	4.0								3.4
42:04.0	2921						I	S										6.1	6.1					6.1
42:19.0	3421					I	S	S									5.0	7.3	3.5					3.5
42:25.0	3621		I	I	S									x	x	5.9								5.9
42:37.0	4021					I	S										6.6	4.6						4.6
42:42.0	4187				I	S	S									4.4	5.3	x						4.4
42:57.0	4687				I	S	S									6.7	6.1	4.4						4.4
43:02.0	4854			I	S	S									x	4.0	4.7							4
43:19.0	5421					I	S										6.3	3.8						3.8
43:26.0	5654							I	I	I									4.1	4.4	4.9			4.1
43:48.0	6387						I	I	I	I								x	x	x	x			x
44:01.0	6821							I	S	S	S								8.5	7.3	7.0	5.6		5.6
44:17.0	7354							I	S										9.2	6.7				6.7
44:20.0	7454	I	S	S	M	M	S	S					3.9	4.4	4.8	5.3	4.1	7.1	7.1					3.9
44:39.0	8087	S	S										4.4	3.9										3.9
44:41.0	8154							I	S										3.5	3.5				3.5
44:42.0	8187	L	L	L									4.7	3.0	5.3									3
45:27.0	9687		I	S										5.3	4.1									4.1
45:31.0	9821							I	I	S	S	S							4.1	4.4	5.3	6.3	3.9	3.9
45:42.0	10187	I	S	S									5.2	4.1	3.0									3
45:56.0	10654									I	S	S									4.0	7.5	6.9	4
46:44.0	12254					I	I	S	S	S							4.0	6.8	5.0	4.1	11			4
46:51.0	12487	I	S	S	S								5.8	5.7	4.0	4.9								4
47:00.0	12787	I	M	S									5.2	8.8	4.6									4.6
47:24.0	13587							I	I										5.5	x				5.5
47:27.0	13687	I	I	I									4.5	5.7	5.8									4.5
47:28.0	13721	I	S										3.5	4.3										3.5
48:11.0	15154				I	S										5.2	3.0							3
48:26.0	15654					I	I										4.1	3.6						3.6
48:37.0	16021					I	S	S									6.6	5.1	4.0					4
49:06.0	16987				I	I										5.6	2.9							2.9
49:10.0	17121				I				I	I	I	I				2.9				4.5	7.3	4.0	5.4	2.9
49:16.0	17321		I	I										5.7	6.5									5.7
49:19.0	17421							I	I	S	S								x	6.5	7.7	5.8		5.8
49:21.0	17487	I	I	I	I								4.4	5.5	3.6	5.0								3.6
49:30.0	17787	S	S	S	S	S							6.1	4.9	4.8	5.7	5.0							4.8
49:43.0	18221	S	S										9.5	4.5										4.5
49:47.0	18354			I	S										6.8	12								6.8
49:48.0	18387			I	S	S	S	S	S	S					3.0	5.9	5.4	9.4	12	x	x			3
I: incipient S: small M: medium L:large																	Peak of breaking							

Breaking Waves
Experiment 8

TIME	DATA																						(rad)
50:01.0	18821					I	I										5.3	3.6					3.6
50:32.0	19854	I	I	S	S								3.1	6.9	5.3	6.6							3.1
50:39.0	20087						I	I	I	I								6.6	5.4	5.5	6.5		5.4
50:41.0	20154	S	S	S	S								5.6	4.2	4.5	3.0							3
50:50.0	20454				I	S										4.8	3.4						3.4
51:06.0	20987			I	S	S	S								9.9	7.5	5.7	x					5.7
51:15.0	21287							I	I	S	S								4.2	6.3	6.9	4.7	4.2
51:24.0	21587					I	S	S									9.5	8.9	8.2				8.2
51:38.0	22054				I	I										4.1	3.5						3.5
51:40.0	22121								I	I	S	S								5.6	5.6	4.3	4.6	4.3
52:02.0	22854						I	S	S									9.6	x	x				9.6
52:46.0	24321	I	I	S	S								6.1	6.2	6.4	6.5							6.1
52:52.0	24521				I	I	S	S	S							4.0	5.4	6.5	5.1	4.6				4
52:55.0	24621	I	I	S	M	M	S	S	S				5.2	3.3	5.7	4.5	5.7	x	3.8	x				3.3
53:10.0	25121					I	I										5.5	8.1						5.5
53:26.0	25654					I	I	I									x	5.1	4.6					4.6
53:59.0	26754	I	S										7.1	4.2										4.2
54:02.0	26854								I	I	I	I								6.0	3.4	5.4	x	3.4
54:08.0	27054	S											7.2											7.2
54:19.0	27421					I	I	I	S	S							4.4	4.1	5.6	5.3	5.1			4.1
54:36.0	27987						I	I	S									3.5	5.3	5.4				3.5
54:44.0	28254						I	I	I									3.7	3.4	3.1				3.1
54:55.0	28621						I	I	S									6.2	5.8	6.7				5.8
54:59.0	28754		I	S	S	S								4.5	4.9	4.6	5.0							4.5
55:01.0	28821								I	I	S	S								6.0	7.1	6.3	5.3	5.3
55:15.0	29287						I	I	S									4.0	x	4.5				4
55:29.0	29754						I	S	S									x	7.1	5.3				5.3
55:43.0	30221						I	I	S									5.5	5.5	x				5.5
55:57.0	30687	S											5.9											5.9
56:01.0	30821				I	I	S									7.5	8.1	7.5						7.5
56:13.0	31221						I	I	S									4.8	7.6	8.7				4.8
56:38.0	32054		I	I	S	M	M	S	S	S				x	5.0	4.8	3.7	3.6	x	5.8	5.5			3.6
I: incipient S: small M: medium L:large																	Peak of breaking							

Breaking Waves
Experiment 9

GAUGE		1	2	3	4	5	6	7	8	9	10	11	1	2	3	4	5	6	7	8	9	10	11	F. dev.
TIME	DATA																							(rad)
12:59.0	751		I	S										6.8	x									6.8
13:01.0	818							I	I										7.2	7.5				7.2
13:02.0	851		I	S										4.1	5.6									4.1
13:22.0	1518	I	S	S									4.1	5.9	3.9									3.9
13:25.0	1618	S											5.1											5.1
13:29.0	1751	I	S	S									4.3	5.4	3.8									3.8
14:10.0	3118					I	I	I									5.3	5.6	3.2					3.2
14:17.0	3351					I	I	S									3.5	4.7	4.8					3.5
14:30.0	3784					I	S										5.2	x						5.2
15:26.0	5651	I	S	S									3.4	7.8	7.1									3.4
15:29.0	5751	S											3.5											3.5
15:57.0	6684		I	I	S	S	M	S						2.9	5.5	5.6	6.8	5.8	3.7					2.9
16:16.0	7318							I	I										3.0	4.5				3
16:34.0	7918		I	I	I	I								4.1	3.9	3.2	3.0							3
16:47.0	8351					I	S	S									6.9	10	5.8					5.8
17:02.0	8851				I											6.3								6.3
17:05.0	8951			I											4.1									4.1
17:06.0	8984	S											5.1											5.1
17:24.0	9584							I	I	S	S								4.0	6.4	4.4	3.4		3.4
18:07.0	11018			I	I	I									4.6	4.5	x							4.5
18:17.0	11351						I	I	I	I								5.0	4.5	4.0	3.8			3.8
18:19.0	11418	S	S	S									10	11	10									10
18:22.0	11518									I	S	S									9.8	6.9	3.8	3.8
18:40.0	12118		I	I	I									3.6	6.5	4.6								3.6
18:43.0	12218								I	I	S	S								7.0	6.6	5.2	3.5	3.5
18:55.0	12618	I	S	M	L	M	M						x	7.3	8.6	8.2	5.0	8.3						5
19:05.0	12951			I	I	S	S	S							x	4.5	4.0	x	3.2					3.2
19:23.0	13551				I											5.2								5.2
19:31.0	13818				I	S										4.6	3.9							3.9
19:37.0	14018					I	I	S	S	S	M	S					x	4.3	6.5	6.2	12	6.7	6.4	4.3
20:08.0	15051							I	I	I									3.5	x	4.8			3.5
20:23.0	15551			I	S	S									6.8	6.1	4.9							4.9
20:44.0	16251		I	I										7.7	4.5									4.5
21:11.0	17151	M	M										7.3	6.6										6.6
21:13.0	17218									I	I										12	6.7		6.7
21:39.0	18084								I	S	S	S								6.1	7.3	5.4	5.6	5.4
22:02.0	18851	I	I	S									4.2	7.4	5.0									4.2
22:04.0	18918								I	I										4.6	2.9			2.9
22:27.0	19684				S	S										3.1	5.5							3.1
22:40.0	20118					I	I	S	S	M							x	4.8	5.5	5.0	4.3			4.3
23:07.0	21018	S	M	L	S								7.2	8.6	7.2	7.9								7.2
23:13.0	21218					I	I	I									5.0	4.5	3.5					3.5
23:36.0	21984	I	S	S									6.1	6.2	4.1									4.1
I: incipient S: small M: medium L:large																	Peak of breaking							

Breaking Waves
Experiment 9

GAUGE		1	2	3	4	5	6	7	8	9	10	11	1	2	3	4	5	6	7	8	9	10	11	F. dev.
TIME	DATA	1	2	3	4	5	6	7	8	9	10	11	1	2	3	4	5	6	7	8	9	10	11	(rad)
23:48.0	22384					I	I	S									5.7	7.0	6.0					6
23:49.0	22418		I	I	I									3.6	x	x								3.6
24:12.0	23184				I	I										5.8	5.0							5
24:13.0	23218							I	I										4.6	4.2				4.2
24:27.0	23684		I	I										4.0	3.3									3.3
24:28.0	23718							I	S										x	3.6				3.6
24:38.0	24051	I	S	M	M								6.0	7.4	3.0	4.0								3
24:47.0	24351				I	S										8.5	6.3							6.3
24:52.0	24518					I	S	S									5.9	7.3	5.1					5.1
25:04.0	24918								I	I	S	S								5.6	5.1	7.0	4.5	4.5
25:17.0	25351				I	I	I	I								4.3	5.1	x	x					4.3
26:04.0	26918	S	M										8.0	5.2										5.2
26:06.0	26984							I	I	S									6.5	6.6	3.7			3.7
26:13.0	27218	I	S	S	S								4.5	6.2	3.4	3.4								3.4
26:16.0	27318									I	S	S									7.5	5.2	3.9	3.9
26:31.0	27818		I	S	S									x	x	x								x
26:33.0	27884							I	I	S									6.4	5.9	7.4			5.9
26:56.0	28651			I	S	S									5.6	5.1	5.3							5.1
27:06.0	28984		I	S	S	M								x	9.1	6.5	5.2							5.2
27:16.0	29318	I	I										x	x										x
27:18.0	29384					I	I										7.9	5.9						5.9
28:02.0	30851						I	I										3.4	7.7					3.4
28:15.0	31284		I	I	I									x	3.6	3.5								3.5
28:27.0	31684		I	S	S	M								8.1	9.3	8.4	9.6							8.1
28:39.0	32084							I	I	I	I								2.9	3.2	5.0	4.3		2.9
28:48.0	32384		I	S	S	S								3.1	10	7.3	9.8							3.1
29:05.0	32951			I	S	S									o	o	o							

I: incipient S: small M: medium L:large Peak of breaking

Breaking Waves
Experiment 10

GAUGE		1	2	3	4	5	6	7	8	9	10	11	1	2	3	4	5	6	7	8	9	10	11	F. dev.
TIME	DATA																							(rad)
30:57.0	287					I	I	S	S	S							5.3	8.3	4.8	6.1	4.0			4
31:11.0	754					I	S	S									4.1	6.0	3.7					3.7
31:22.0	1121				I	I	S	S	S	S						3.9	6.2	5.9	6.4	3.1	3.5			3.1
31:37.0	1621		S	S										7.4	4.1									4.1
31:39.0	1687							I	I	I	I	I							6.3	7.5	19	6.5	x	6.3
31:42.0	1787			I	I	I									4.4	3.2	4.2							3.2
31:47.0	1954		I	I	I									3.2	4.6	x								3.2
32:20.0	3054			I	I										7.2	3.8								3.8
32:42.0	3787					I	I	I									4.6	6.1	5.6					4.6
32:46.0	3921			I	S										5.8	3.8								3.8
32:56.0	4254					I	I	S	S								4.1	12	10	5.6				4.1
33:11.0	4754		S	S										7.8	9.6									7.8
34:23.0	7154						I	I	I									6.9	10	7.9				6.9
34:43.0	7821						I	S	S	S								7.0	5.7	4.5	6.9			4.5
34:45.0	7887	I	S	M	S								4.2	6.9	7.2	5.0								4.2
34:53.0	8154	I	S	S									5.1	4.4	4.0									4
35:21.0	9087						I	I	S									5.0	5.9	5.3				5.3
35:56.0	10254	S	S										4.1	3.7										3.7
35:39.0	9687								I	I	S	S								5.7	7.2	5.7	3.5	3.5
35:42.0	9787				I	I	I									6.3	6.5	4.2						4.2
35:54.0	10187								I	I	S									6.8	9.2	9.4		6.8
36:14.0	10854	S											4.7											4.7
36:17.0	10954							I	I	I									4.7	6.1	4.9			4.7
36:35.0	11554					I	I										6.3	4.0						4
36:58.0	12321			I	S	S									3.2	4.8	3.5							3.2
37:06.0	12587	I	S	I									3.1	4.5	3.1									3.1
37:18.0	12987				I	I	S	S	S							6.2	7.0	4.7	7.9	3.0				3
37:32.0	13454	S	S										5.6	4.7										4.7
37:42.0	13787							I	I	I	S								x	x	x	x		x
37:59.0	14354			I	S	S	S								6.8	8.2	6.8	7.2						6.8
38:08.0	14654	S	S										4.3	5.8										4.3
38:10.0	14721								I	I	I	I								7.0	3.8	5.9	3.2	3.2
38:35.0	15554								I	I	S	S								5.3	8.5	7.1	10	5.3
38:44.0	15854							I	I										x	x				x
38:54.0	16187				I	S	S	S								6.7	6.1	5.1	5.4					5.1
39:02.0	16454			I	I	I									5.4	4.4	3.4							3.4
39:10.0	16721	I	S										7.6	6.7										6.7
39:12.0	16787						I	S	S									7.7	7.2	3.8				3.8
39:21.0	17087			I	I										8.3	4.8								4.8
39:37.0	17621				I	S	S									6.6	6.0	4.3						4.3
39:42.0	17787			I	I	I									3.2	4.7	3.7							3.2
39:57.0	18287						I	S										6.3	5.3					5.3
40:08.0	18654		I	S										7.7	6.0									6

I: incipient S: small M: medium L:large Peak of breaking

Breaking Waves
Experiment 10

GAUGE		1	2	3	4	5	6	7	8	9	10	11	1	2	3	4	5	6	7	8	9	10	11	F. dev.
TIME	DATA																							(rad)
40:10.0	18721							I	S	S									8.5	7.2	4.9			4.9
40:28.0	19321				I	S										7.4	5.6							5.6
40:31.0	19421	M	S										6.5	7.8										6.5
40:34.0	19521									I	S	S									6.3	3.8	x	3.8
40:47.0	19954		I	S	S									5.1	6.2	4.8								4.8
41:00.0	20387					I	I	I	I								5.2	3.9	4.7	x				3.9
41:08.0	20654	I	M	S									6.2	9.5	4.3									4.3
41:21.0	21087						I	S	S	S	S	S						3.9	5.6	6.2	3.2	x	4.2	3.2
41:31.0	21421		I	I										4.8	4.4									4.4
41:37.0	21621							I	I										5.8	x				5.8
41:49.0	22021	S											4.7											4.7
42:03.0	22487					I											4.0							4
42:09.0	22687				I	S	S	S								5.4	6.1	6.7	4.4					4.4
42:15.0	22887	S											5.3											5.3
42:18.0	22987								I	I	S									4.5	6.4	4.8		4.5
42:20.0	23054	S	S										5.5	3.4										3.4
42:33.0	23487	I	S										8.8	7.2										7.2
42:49.0	24021	I											5.6											5.6
43:18.0	24987				I	I	S									3.9	x	4.7						3.9
43:28.0	25321		I											7.9										7.9
43:37.0	25621	I	I	S	M	S							5.0	6.4	7.1	4.9	7.3							4.9
43:44.0	25854	S	S	S									9.8	8.3	6.7									6.7
44:17.0	26954	S											6.8											6.8
44:25.0	27221				I	S										7.8	4.2							4.2
44:26.0	27254	I	S										6.5	8.4										6.5
44:42.0	27787						I	S	S									6.5	4.4	5.2				4.4
44:51.0	28087		I											x										x
44:59.0	28354			I	I	S	S								4.6	8.2	7.9	6.0						4.6
45:09.0	28687	I	S										6.4	3.2										3.2
45:39.0	29687				I	I	S	M								6.2	8.9	6.5	10					6.2
46:13.0	30821	I	I	I									3.5	x	4.5									3.5
46:15.0	30887							I	S										5.3	3.8				3.8
I: incipient S: small M: medium L:large																Peak of breaking								

APPENDIX B

PHASE-TIME METHOD SEQUENCE

[gauge,dt]=readfile(exp);	Reads the data
npts=max(size(gauge(d,:)));	Reads the amount of data points at the gauge d
gat=gauge(d,x);	Creates gat as the wave elevation data of gauge d
Hgat=hilbert(gat);	Calculates the Analytical function from the original time-series and its Hilbert transform
theta=angle(Hgat);	Calculates the Angle (phase) in radians
thetaa=unwrap(theta);	Unwraps the phase
thetab=detrend(thetaa)	Detrends the phase
fr=diff(thetab)./diff(t);	Computes the frequency
fr=[fr 0.];	Restores the size by adding a 0 at the end
Plot(fr);	Plot the result

APPENDIX C

MATLAB PROGRAM FOR

DEEP WATER BREAKING WAVE DETECTION

```
exp= ['wt',int2str(j),'.dt1'];          gives to exp the data of experiment j
[gauge,dt]=readfile(exp);               reads the data of experiment j

npts=max(size(gauge(d,:)))              gives the number of data points in gauge d

x= 1:npts;
t=x*dt;
gat=gauge(d,x);                         defines gat as the data vector for gauge d

Hgat=hilbert(gat);                      creates the analytical function (ψ)
hilbe=imag(Hgat);                       gives the Hilbert transform
theta=angle(Hgat);                      calculates the phase angle
thetaa=unwrap(theta);                   unwraps the phase
thetab=detrend(thetaa);                 detrend the phase
fr=diff(thetab)./diff(t);               calculates the frequency
fr= [fr 0.];                            restore the size of the frequency

for i=x
std(i)=0.095;                           First parameter: 1.5 times the standard dev.
cst(i)=3.1;                             Second parameter: Fdev=3.1 radians
end

x0=[gat(1),gat];                        creates 2 vectors x0,x1 from the original gat
x1=[gat,gat(npts)];
ind=[find((x0<0).*(x1>=0))];            defines the upcrossing points
nc=length(ind)-1;                       gives the number of upcrossing points

ffr=[];
ffr=fr;                                 defines ffr as fr
```

```
for i=1:nc;
        [zz,vv]=max(gat(ind(i):( (ind(i)+ind(i+1))/2));      defines the peak of
                                                              each wave and its
                                                              location in the data
        [ma,mm]=max(fr(ind(i):( (ind(i)+ind(i+1))/2));       defines the peak of
                                                              frequencydeviation for each
                                                              wave and its location


        if zz>0.097
                if ma>3.1
                        lis=[lis,vv+ind(i)-1,ma];            lists the waves detected in lis

                end
        end
end


for i=1:nc;
[zz,vv]=max(gat(ind(i):ind(i+1)));    calculates the peak of each wave, and gives its
                                      position in the data.

if zz<0.095
ffr(ind(i):ind(i+1))=zeros(1,ind(i+1)-ind(i)+1);      first parameter
end                                                   frequency=0 for the waves under 1.5
                                                      times the standard deviation


for ii=ind(i):ind(i+1);
        if gat(ii)<0
                ffr(ii)=0;
        end
end

gat(pd)=-0.18;
gat(pf)=-0.18;

%plots the wave elevation, frequency for the waves under 1.5 stddev, the threshold of
%detection
```

```
figure
fill(xx,gat(xx)*40,'y');
hold on;
plot(xx,gat(xx)*40,'g',xx,ffr(xx),'w',xx,std(xx)*40,'m--',xx,cst(xx),'w:');
axis([pd pf -10 12]);

%plots the unwrapped phase
figure
plot (xx,thetaa(xx),'m');
title(['Unwrapped Phase function, exp.',int2str(j),' , gauge ',int2str(d)]);
xlabel('Time, (dt=0.03s)');
ylabel('Phase (radians)');

%plots the deviation of the local frequency
figure
plot (xx,fr(xx),'m');
title(['Deviation of the Local Frequency, exp.',int2str(j),' , gauge ',int2str(d)]);
xlabel('Time, (dt=0.03s)');
ylabel('Frequency deviation (radians)');
```

APPENDIX D

DETECTION MODEL, EXPERIMENT 4, GAUGE 5

441 *7* 6855 *5* 728 *4* 981 *5* 2251 *8* 2843 *6*

3271 *4* 3438 *4* 3715 *8* 4308 *6* 5046 *5* 5486

7 6502 *4* 71197 *8* 7507 *4* 7603 *5* 8106 *7*

9661 *8* **9876 *4*** 10266 *4* 11391 *5* 12033 *5* 12565

11 **12977 *5*** 13865 *5* 14133 *7* 14705 *3* 16231 *4*

18643 *6* 19033 *5* 19564 *6* 19872 *5* 19952 *6* 20291

6 21036 *11* 21421 *4* **21822 *3*** 22187 *6* 23340 *5*

24846 *4* **25186 *4*** 25344 *3* 25452 *6* 26425 *3* 26852

5 28003 *7* 28149 *4* 29033 *8* 29402 *5* 29674 *5*

29785 *5* 30857 *6* 31391 *4* 32496 *4*

The numbers indicate which waves in the data are detected by the model (peak of breaking).

The numbers in *italic* indicate the frequency deviation of the wave.

The numbers in **bold** and underline indicate the false detection.

VITA

Charles-Alexandre Zimmermann was born in Strasbourg, France, on May 10, 1974. He lived most of his life in Paris, France. In 1992, Charles started his college education at the preparatory school Fénelon in Paris. He was then accepted at the civil engineering school (grande école) "l' Ecole Spéciale des Travaux Publics (ESTP)" in Paris in 1994. He graduated with a Master of Science in Civil Engineering in 1997. In August 1996, Charles came to Texas A&M University where he joined the Ocean Engineering program in the Civil Engineering department. He was enrolled in the Master of Science program to graduate in May 1998. During his stay at Texas A&M University he has been employed as a research assistant at the Offshore Technology Research Center, and was member of the Executive committee of the OTRC student forum.

Charles-Alexandre can be reached at his permanent address in France:

63 rue Nationale
92100 Boulogne
France
phone/fax: 011-33-1 46 09 13 47

or through the:

Offshore Technology Research Center
1200 Mariner Drive
College Station, TX 77845

266.C

Detection of Deep Water Breaking Waves

by

Charles-Alexandre Zimmermann

1998

NSF# CDR-8721512

3/98A9675

For more information contact:

Offshore Technology Research Center
Texas A&M University
1200 Mariner Drive
College Station, TX 77845
(409) 845-6000

or,

Center for Offshore Technology
The University of Texas at Austin
2901 North IH 35, Suite 101
Austin, Texas 78722
(512) 471-3753

DETECTION OF DEEP WATER BREAKING WAVES

A Thesis

by

CHARLES-ALEXANDRE ZIMMERMANN

Submitted to the Office of Graduate Studies of
Texas A&M University
in partial fulfillment of the requirements for the degree of

MASTER OF SCIENCE

May 1998

Major Subject: Ocean Engineering

ABSTRACT

Detection of Deep Water

Breaking Waves. (May 1998)

Charles-Alexandre Zimmermann, B.S., Ecole Speciale des Travaux Publics;

Co-Chairs of Advisory Committee: Dr. Jun Zhang
Dr. Richard Seymour

Records of deep water sea surface elevation, even taken at high sampling rates, do not provide evidence for which waves in the record are breaking. Although a visual observation of steep random waves clearly shows even the beginning of a breaking event, the white capping and collapse of the front face of a breaking wave do not appear in any meaningful way in the output of an elevation gauge. Much research has been conducted in an attempt to find a way of detecting breaking events in an wave elevation record. Some criteria have been advanced, but most of them show quite low accuracy. *Huang et al.* [1992] suggested that an analytical method, which they called the Phase-Time Method, might be used to detect breaking events. This study evaluates the power of the Phase-Time method in breaking wave detection. Large scale laboratory experiments are used to obtain a quality data set under a variety of deep water wave conditions. The physics of the Hilbert transform used in the Phase-Time Method are studied, and the method is explored as a breaking wave detection tool. A model of deep water breaking wave detection is developed and its limits are stated.

ACKNOWLEDGMENTS

This research investigation was supported by the Offshore Technology Research Center (OTRC), a National Science Foundation Engineering Research Center, through grant # CDR-872152.

I would like to thank Dr. Richard Seymour, Co-Chair of the committee for offering me the opportunity of working on this research, and helping me with his experience in conducting this very interesting investigation. I would also like to thank Dr. Jun Zhang who Co-chaired the committee for providing valuable insights into the development of the model, and for helping me in clarifying certain aspects of the study.

The experimental part of the project was conducted by Eustorgio Meza (Toyo) , Mr. Peter Johnson and the OTRC technical staff whose support was greatly appreciated. I would like to specially thank Toyo for his help.

The author further acknowledges Dr. Guy Battle the 3rd, committee member for his contribution to this research effort.

TABLE OF CONTENTS

Page

CHAPTER Page

LIST OF FIGURES

FIGURE Page

FIGURE Page

LIST OF TABLES

TABLE Page

CHAPTER I

INTRODUCTION

Breaking waves in the ocean

Wave breaking may occur over a large range of scales, especially in deep water. Deep water, in the context of wave studies, is defined as deep enough so that the surface waves are unaffected by the direct effects of the variation of the sea floor. Direct observations are still very important in the study of this complex breaking phenomenon because only the visual aspect of a breaker can, at present, define its type of breaking.

Statistics of breaking waves are critical to dissipation estimates in wave growth models. Breaking is a dominant dissipation term in models for wave generation and propagation, yet there are few observations in deep water of these statistics. Therefore, the breaking term in present models contains a high degree of uncertainty. The need for understanding and predicting the breaking events from wave gauge data is thus very important.

In the past, much research have been devoted to finding a way of detecting these breaking events in a wave elevation record. Particularly in the past 20 years, many criteria for the detection of wave breaking events have been proposed, but none of them

---

This thesis follows the style and format of the *Journal of Geophysical Research.*

proved to be efficient. Moreover, these criteria are very often difficult to use. In fact, there is still no generally acceptable method for detecting these breaking events, even after all the research that has been undertaken. Some of these studies have been concerned primarily with breaking detection and statistics, while other studies have focused on investigating basic properties of breaking waves.

Wave breaking in deep water can be classified in the following two categories:

- The most dramatic breakers are plunging breakers where the breaking commences by the wave overturning and the formation of a sheet of water which plunges down into the water causing splashes, and eddies. These plunging breakers are common on beaches but do not occur often in deep water.

- The other breakers are the spilling breakers. From their initiation, some air bubbles and water fall down the front face of the wave. The wave is breaking continuously, losing energy as its front face breaks in a much less dramatic manner than the plunging breaker. These breakers are 'spilling' along their crest, prohibiting the appearance of a plunging breaker. They can appear either in deep water waves or in shoaling waves approaching the shore.

Current status of the detection methods

An overview of the deep water breaking wave detection methods was provided by *Banner and Peregrine* [1993]. They describe the different methods of detection used so

far, the theoretical studies of wave hydrodynamics relevant to breaking and they state the different problems regarding these detecting method.

A basic characteristic, as it is generally recognized, is that an individual wave breaking event usually starts when water particles near a wave crest develop a velocity in the wave propagation direction sufficiently large for them to fall down the front of the wave. However, the surface fluid speed is difficult to measure in the field and such a characteristic is useless in the field.

The traditional criterion for wave breaking is that horizontal water velocities in the crest must exceed the speed of the crest profile. This appears self-evident, but since the crest shape is changing there is often no precisely relevant crest velocity. The surface fluid speed being difficult to measure in the field makes this criterion quite unusable.

The traditional methods used for detecting the breaking are:

- The Optical Detection Methods: Modern video recording and image processing techniques have been particularly useful for whitecap cover measurements.
- Wave Gauge Detection Method: *Holthuijsen & Herbers* [1986] demonstrated the inadequacy of using a simple local wave slope criterion. *Longuet-Higgins & Smith* [1983] and *Thorpe & Humphries* [1980] developed a method relying on the rapid jump in surface elevation at the leading edge of the spilling region of a breaker. This method proved to give much lower breaking probabilities than there was in reality.

- Radar Methods: Narrow-beam Doppler radars are used to detect large-scale breaking events. These radars measure the significant increase in scatterer speed within breaking events [*Keller et al.*, 1986].

- Acoustic Methods: *Snyder & Kennedy* [1983] studied the acoustic output from large-scale whitecaps to trigger a rapid sequence of photographs.

- *Longuet-Higgins* [1969] presented a simple statistical model for the loss of energy by wave breaking based on a crest downward acceleration threshold of 0.5g for the sharp-crested limiting Stokes wave.

- Finally some studies have started to investigate the use of the local wavetrain properties derived from the Hilbert transform of the wave elevation signal [*Melville*, 1982; *Hwang et al.*, 1989; *Huang et al.*, 1992].

The Phase-Time Method

Huang et al. [1992] studied the local properties of the ocean surface waves by applying an analytical method which they called the Phase-Time Method (PTM) to their data. This PTM consists in using the Hilbert transform of the elevation time-series to obtain, after a few operations, a time-series of the deviation of the local frequency from the mean frequency of the record. This is done by first constructing an analytical function based on the original time-series and its Hilbert transform. Then we construct a time history of the local phase function of this analytical function. By unwrapping this phase function, and then differentiating it, we obtain a valuable time-dependent information on

the local frequency of the record. This method will be clearly explained in the next chapters. *Huang et al.* showed that by using this method, we can gain a fresh view of the wave data. Furthermore, they implied that a break in the phase function could be used as an indicator of wave breaking, noting that the existence of this type of breaking wave criterion had never been seriously investigated.

Finally, *Griffin et al.* [1996] performed some experiments to study the kinematics and dynamic evolution of deep water breaking waves. They showed that the PTM provides some new insight into the local properties of the unsteady wave breaking. They reported that the instantaneous Hilbert amplitude (which is defined as the amplitude of the analytic function formed by adding the wave elevation time-series and its Hilbert transform) clearly focuses on the asymmetry between the front and rear faces of the wave. They also pointed that the evolution of the Hilbert frequency of the packet toward breaking in the wave channel shows nearly constant behavior for the non breaking waves, slight growth for the spilling breakers and finally sharp growth for fully plunging breakers. However, they do not provide any kind of detection model, or physical approach for this Phase-Time Method.

Objectives

This research is conducted in order to explore the possibility of validating a deep water breaking wave detection model based on the Phase-Time Method. We evaluated the power of the PTM approach to breaking wave detection. Different objectives were met in order to obtain satisfactory results in our research:

- Obtain a quality data set under a variety of deep water wave conditions with a substantial number of breaking waves and video documentation to discriminate the breaking events visually and evaluate the type of breaking.

- Understand the physics related to the Hilbert transform and to the time-series of the local deviation of the frequency obtained by using the Phase-Time Method.

- Apply the Phase-Time Method to the acquired data and explore this method as a detection method for breaking waves.

- Develop and validate a model for breaking detection.

Procedure

The first step of the research is the data gathering. A large number of deep water random wave experiments were conducted in the Offshore Technology Research Center Model Basin. A large linear array of wave staff was employed with multiple video cameras to record breaking events along the array. The data was acquired from 12 experiments with a range of significant heights and periods. The experiments will be described in the next chapter. The implementation of the video cameras records allow us to have a visual record of the breaking waves in each of the experiments.

The next step is to study the physics of the Hilbert transform in order to understand how it can be used in detecting the breaking events in the data set. This allows us to eventually understand the results obtained when we apply the Phase-Time Method to the

data, and see which are the criteria we need to add to the model to make it practical and accurate. This would also help in understanding the results of past research in this domain.

The Phase-Time Method was applied to obtain time-series of the deviation of the local frequency. By analyzing the data from the experiments, and by using the video records as a tool to check and distinguish the breaking waves and non-breaking waves, we tried to find some characteristic patterns in this frequency signal which are related to the wave breaking. These characteristics are potentially useful in developing a detection model.

If some characteristic patterns are found and a model can be developed, its skills to detect the breaking waves need to be evaluated in order to validate the model. Finally the limits of the model need to be stated and its range of application determined.

CHAPTER II

EXPERIMENTAL DESIGN

This section describes the development of the experimental plan which provided the data for the Phase-Time Method evaluation. A large number of deep water random wave experiments (12 in total) were conducted at the Offshore Technology Research Center Model Basin. A large array of wave staffs was employed with multiple video cameras. The overall objective of the experimental study was to obtain a quality and realistic data set under a variety of deep water wave conditions with a substantial number of breaking events and a video documentation to allow the evaluation of the Phase-Time Method.

Experimental objective

This experiment appears to be unique and was designed with the goal of developing a model for detecting the breaking events under deep water conditions.

The principal goal of the experiment was to acquire a data set in which there are a significant number of clearly-identifiable wave breaking events that occur in plane (non-directional) waves with spectra similar to the JONSWAP type. The data set should include as many high frequency wave wire measurements sampled at 30-50 Hz as possible. The occurrence of breaking will be based upon visual observation of time-synchronized video records of the surface in the vicinity of each gauge.

Three different wave trains should be employed. Their spectra are similar in shape (JONSWAP type) but peaked at different frequencies, covering the broadest range possible while still generating reasonable waves. Runs should be as long as possible. Each setting should be replicated three times. The amplitudes should be adjusted so that there is significant breaking (about 10% of the waves) in the zone where the wave gauges are situated.

Model test facility

The experiment was conducted at the Offshore Technology Research Center's model test basin at Texas A&M University (College Station, TX). This facility is the only one in the United States to have the capability of testing deep water Offshore Structures without modification of the vertical scales.

The wave basin (see Figure 1) is 45.7 m (150 ft) long and 30.5 m (100 ft) wide, with a depth of 5.79 m (19 ft). The pit is located in the center of the basin. Its dimensions are 6.10 m by 9.14 m (20 by 30 ft) with a depth up to 16.76 m (55 ft). Observation windows are located at the West, North and East sides of the basin. These windows are approximately 3 m (10 ft) below the water surface and provide an unobstructed view of the entire basin. However, the pit is not really visible from these windows. The water in the basin is clear and it is very easy to see the wave absorber at the South end from the observation window at the North end about 35 m (115 ft) away. The South side of the basin contains a progressive vertical wave absorber. A wave maker with 48 individually controlled wave panels is installed at the North end of the basin. The wave panels are

servo-controlled, each panel has a linear actuator and can be programmed individually. The drive signal for each wave board is created using GEDAP software, software specially developed for model basin testing by the National Research Council of Canada. A bridge spans the width of the tank and can traverse the basin in a North-South direction. The bridge is frequently used to mount equipment. The basin also allows the creation of currents and winds by utilizing variable speed pumps and fans. The basin and wave maker allow the generation of deep water waves within the range of frequencies between 0.3 hz (wave height of 70 cm) and 2 hz (wave height of 5mm). See Figure 2 for a description of the wave maker performance envelope.

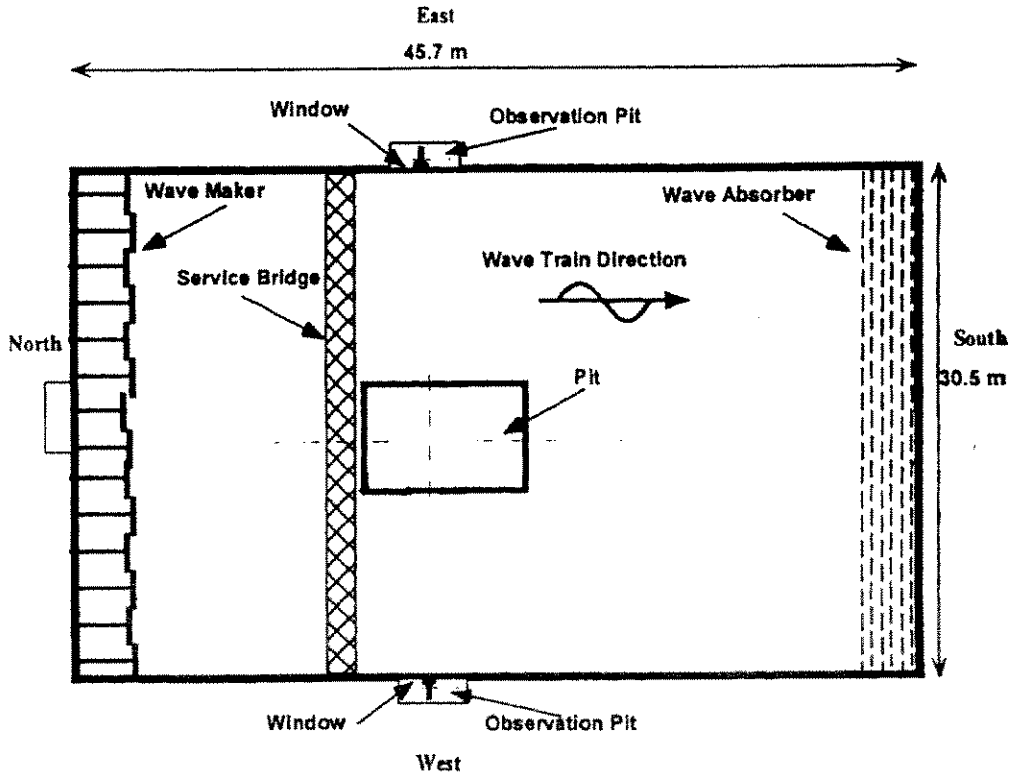

Figure 1. Plan view of the experimental basin.

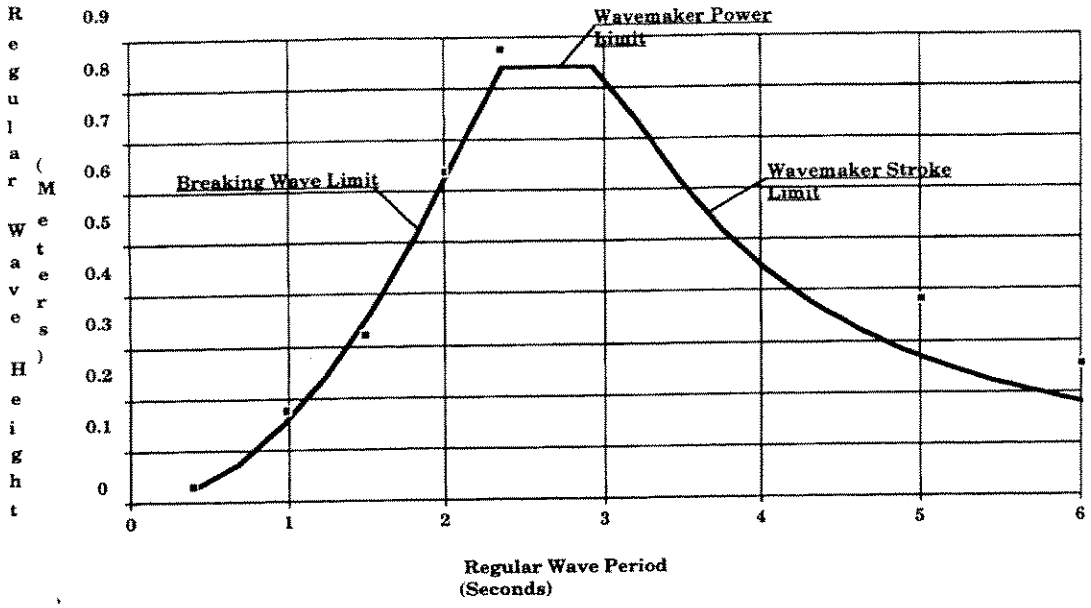

Figure 2. Regular wave height performance envelope.

Experimental setup

Eleven gauges spaced 75 cm apart were used to insure that a breaking event would actually be captured. That is, the spacing was such that it was not possible for the principal portion of a wave breaking event to occur entirely between two gauges. This took some experimentation to determine the best spacing. Putting gauges too close together obviously reduces the number of events that will be captured in a record. It was necessary to adjust the spacing in proportion to the wave length of the dominant wave. The wave wires were clearly identified so that they could be easily picked out of a video record. This required the use of 2 cameras, displayed on a split screen to allow the visualization of the entire array of gauges. Also, the video documentation contained a time signal in a manner to allow easy identification of the particular time history of elevation at each gauge. To prevent any interference of the waves by large numbers of

wave gauges in a small space, they were sequentially offset in the East-West direction a distance equal to their spacing in the North-South direction.

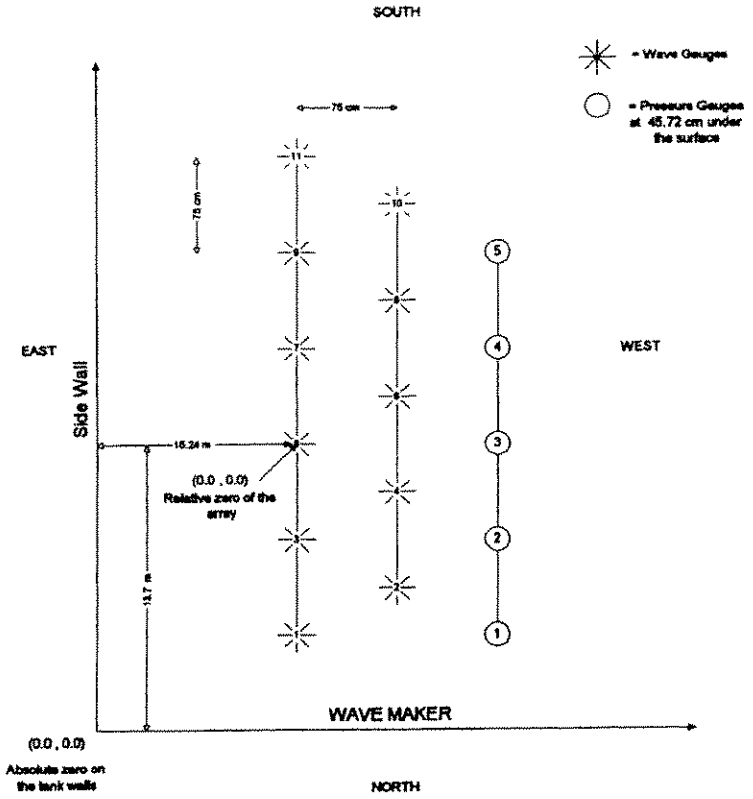

Figure 3. Experimental setup.

The breaking was set to take place 13.7 m away from the wave maker. The experimental plan is described in Figure 3. From our past experiences (measuring pressure under breaking waves), the expected distance in which a wave should break is about 1.8 - 2.5 m (assuming that the process of breaking is the same for every experiment). Since the largest waves created have a period of 2 sec., with a wave length of 6.25 meters and a wave celerity of 3.123 m/sec, it means a breaking process of around 0.6 - 0.8s.

From the above, the proposed distance that should be covered by the gauges was 3 meters, which is also half of the wave length of the largest waves studied. After 3 experiments, the distance covered by the gauges was increased to 4.5 m in order to allow the capture of more breaking events. Two arrays of wave gauges (6 on the first one and 5 on the other one) were installed parallel to each other, with a distance between two gauges of the same array of 75 cm (see Figure 4 and Figure 5). The transverse distance between the 2 arrays is also 75 cm, and finally an array of five pressure gauges is set again 75 cm away from the second array. With this experiment setup, two consecutive gauges are separated by 37.5 cm as seen on Figure 3.

Data acquisition

Three different wave trains were tried at the beginning. The characteristics of these wave trains were defined in terms of the significant wave height and peak frequency in a JONSWAP spectrum. Nine other wave trains were run with different significant heights in order to create even more breaking events. Thus the data was acquired from these 12 runs of experiment, with a range of significant heights and periods. Each experiment had a duration of approximately 16 min with a sampling rate of 33 Hz. The characteristics of each experiment are given in Table 1 (the mean period, frequency and height were calculated using the upcrossing method). These experiments showed a very satisfying number of breaking events, very well distributed in the array of 11 gauges. Table 2 shows the percentage of breaking waves and the amount of incipient (I), small (S), medium (M) and large (L) (see chapter IV) breaking at the gauges for each experiment.

Figure 4. Picture of the 11 gauges array (from the North-East side).

Figure 5. Picture of the 11 gauges array (from the East side).

Table 1. Experiments Characteristics

Experiment	Mean T (sec)	Peak T (sec)	Tm/Tp	Mean F (Hz)	Peak F (Hz)	Peak F (rad)	Mean A (m)	Mean H (m)	H 1/3 (m)
wt1-001	1.43	1.6	0.89	0.70	0.63	3.93	0.07	0.14	0.23
wt2-001	1.58	1.8	0.88	0.63	0.56	3.49	0.10	0.18	0.3
wt3-001	1.71	2	0.86	0.58	0.50	3.14	0.10	0.19	0.32
wt4-001	1.44	1.6	0.90	0.69	0.63	3.93	0.08	0.15	0.26
wt4-002	1.42	1.6	0.89	0.70	0.63	3.93	0.08	0.15	0.26
wt5-001	1.61	1.8	0.89	0.62	0.56	3.49	0.11	0.20	0.33
wt6-001	1.76	2	0.88	0.57	0.50	3.14	0.12	0.22	0.38
wt6-002	1.75	2	0.88	0.57	0.50	3.14	0.12	0.22	0.38
wt7-001	1.6	1.8	0.89	0.63	0.56	3.49	0.11	0.19	0.33
wt8-001	1.53	1.7	0.90	0.65	0.59	3.70	0.10	0.17	0.3
wt9-001	1.53	1.7	0.90	0.65	0.59	3.70	0.10	0.17	0.3
wt10-001	1.52	1.7	0.89	0.66	0.59	3.70	0.09	0.17	0.3

Table 2. Breaking Waves Distribution

Experiment	H 1/3 (m)	Breaking (%)	I	S	M	L
wt1-001	0.23	10.42	92	90	27	9
wt2-001	0.3	13.42	84	102	51	22
wt3-001	0.32	10.27	67	77	25	6
wt4-001	0.26	9.8	98	100	32	4
wt4-002	0.26	9.7	63	94	6	0
wt5-001	0.33	12.47	81	97	30	11
wt6-001	0.38	11.84	78	88	23	4
wt6-002	0.38	11.25	100	84	20	2
wt7-001	0.33	8.6	100	94	28	7
wt8-001	0.3	7.9	119	114	8	3
wt9-001	0.3	8.5	111	78	13	2
wt10-001	0.3	8.8	113	95	5	0

Application of the data

The first question answered with these data was the evaluation of the Phase-Time Method and the approval of the concept of this method as a means of detecting breaking in a surface elevation record. The data was used in order to develop a model to detect breaking waves and to validate it.

Finally, we had to determine how slowly the record can be sampled without losing the ability to detect the breaking using the model. This was done by testing the model on decimating time-series coming from the original data set.

CHAPTER III

THE PHASE-TIME METHOD

In this chapter the physics of the Hilbert transform and the Phase-Time Method are studied in order to understand how this method can be used in detecting the breaking events in the data set. By understanding what this frequency signal obtained from the method involves, we may have an idea of the capability of these methods, and we may find those criteria needed to obtain a quality detection model. This will also allow us to understand eventually the results obtained in previous research in this domain. There appears to be no clear explanation of the physics of this method or of the Hilbert transform in any paper related to this topic.

The Hilbert transform

The Hilbert transformations are presently used in various ways. A clear description of this transform is described in the Transforms and Applications handbook by *A.D. Poularikas* [1996].

Since the 1890s, the complex notation of harmonic signals in the form of Euler's equation $\exp(jwt)= \cos(wt)+j\sin(wt)$ (1)

has been used in various engineering aspects, and is commonly applied to various theoretical systems. This complex notation was introduced before Hilbert derived his

transformations. However, sin(wt) is the Hilbert transform of cos(wt) and exp(jwt) is the precursor of the analytic signals.

The concept of the analytical signals of the form $\psi(t) = u(t) + jv(t)$ where v(t) is the Hilbert transform of u(t), is now widely used in the theory of signals and systems. The Hilbert transformation finds many applications in digital signal processing.

The Hilbert transformation of a one-dimensional real signal (function) u(t) is defined by the principal integral:

$$v(t) = \frac{-1}{\pi} P\int_{-\infty}^{\infty} \frac{u(\eta)}{\eta - t} d\eta = \frac{1}{\pi} P\int_{-\infty}^{\infty} \frac{u(\eta)}{t - \eta} d\eta \qquad (2)$$

and the inverse Hilbert transformation is :

$$u(t) = \frac{1}{\pi} P\int_{-\infty}^{\infty} \frac{v(\eta)}{\eta - t} d\eta = \frac{-1}{\pi} P\int_{-\infty}^{\infty} \frac{v(\eta)}{t - \eta} d\eta \qquad (3)$$

where P stands for the Cauchy principal value of the integral. The integral defined in (2) and (3) are improper because the integrand goes to infinity for η=t. Therefore the integral is defined alternatively as the Cauchy principal Value (P) of the form

$$v(t) = \lim_{\substack{\varepsilon \Rightarrow 0 \\ A \Rightarrow \infty}} \frac{-1}{\pi} \left(\int_{-A}^{-\varepsilon} + \int_{\varepsilon}^{A} \frac{u(\eta)}{\eta - t} d\eta \right) \qquad (4)$$

The accuracy of this numerical integration increases with smaller sampling intervals and larger values of A.

The Hilbert transform was originally derived by Hilbert in the frame of the theory of analytic functions and its theory is closely related to Fourier transformation of signals of the form:

$$U(\omega) = \int_{-\infty}^{\infty} u(t) e^{-j\omega t} dt \qquad \text{where } \omega = 2\pi f \tag{5}$$

$U(\omega)$ is the Fourier spectrum of the signal u(t) and $f=\omega/2\pi$ is the Fourier frequency. The inverse of the Fourier transformation is

$$u(t) = \int_{-\infty}^{\infty} U(\omega) e^{j\omega t} df \tag{6}$$

The pair of functions u(t) and $U(\omega)$ are called a Fourier pair. The pair u(t) and v(t) form a Hilbert pair of functions. The main characteristic of the Hilbert transform is that the transform does not change the domain, contrary to many other transforms. For example in our case, a time-series function is transformed in a function of the same variable t, therefore another time-series is obtained. The Fourier transformation changes a function in the time domain into a function in the frequency domain. The pairs of transforms can be denoted:

$$u(t) \overset{F}{\longleftrightarrow} U(\omega) \tag{7}$$

$$u(t) \overset{H}{\longleftrightarrow} v(t) \tag{8}$$

The Fourier transform of the kernel of the Hilbert transform which is $\Theta(t)=\frac{1}{\pi t}$ is -j sgn(ω) where sgn(ω) is defined as follows:

$$\mathrm{sgn}(\omega)=\begin{cases}+1 & \omega>0\\ 0 & \omega=0\\ -1 & \omega<0\end{cases} \tag{9}$$

Therefore, the properties of the Fourier transform yield to the spectrum of the Hilbert transform:

$$v(t)\xleftrightarrow{F}V(\omega)=-j\,\mathrm{sgn}(\omega)U(\omega) \tag{10}$$

which means that the spectrum of the signal u(t) should be multiplied by the operator - j sgn(ω) which is also called Hilbert transformer. This relation enables the calculation of the Hilbert transform using the Fourier transform and its inverse from the original time-series, using the following procedure:

$$u(t)\xrightarrow{F}U(\omega)\xrightarrow{-j\,\mathrm{sgn}(\omega)}V(\omega)\xrightarrow{F^{-1}}v(t) \tag{11}$$

where F and F^{-1} denote the Fourier and inverse Fourier transformations respectively.

A real signal u(t) may be written in terms of analytic signals

$$u(t)=\frac{\Psi(t)+\Psi^{*}(t)}{2} \tag{12}$$

and its Hilbert transform is

$$v(t) = \frac{\Psi(t) - \Psi^*(t)}{2j} \tag{13}$$

where $\Psi(t)$ is the analytic signal (or function) defined by

$$\Psi(t) = u(t) + j\, v(t) \tag{14}$$

where u(t) and v(t) are continuously differentiable and $\Psi^*(t)$ denotes the conjugate of $\Psi(t)$.

It is now obvious that these notations are related to the widely used Euler's equation and provide a generalization of Euler's formulae:

$$\cos(\omega t) = \frac{e^{j\omega t} + e^{-j\omega t}}{2} \tag{15}$$

$$\sin(\omega t) = \frac{e^{j\omega t} - e^{-j\omega t}}{2j} \tag{16}$$

where $e^{j\omega t} = \cos(\omega t) + j\sin(\omega t)$, and $e^{-j\omega t} = \cos(\omega t) - j\sin(\omega t)$.

In general, the Fourier image of u(t) is a complex function

$$U(\omega) = U_{\mathrm{Re}}(\omega) + jU_{\mathrm{Im}}(\omega) \tag{17}$$

The multiplication of the Fourier image by the operator -j sgn(ω) changes the real part of the spectrum to the imaginary one and vice versa. The spectrum of the Hilbert transform is

$$V(\omega) = V_{\mathrm{Re}}(\omega) + jV_{\mathrm{Im}}(\omega) \tag{18}$$

where

$$V_{\mathrm{Re}}(\omega) = -j\,\mathrm{sgn}(\omega)[jU_{\mathrm{Im}}(\omega)] = \mathrm{sgn}(w)U_{\mathrm{Im}}(\omega) \tag{19}$$

$$V_{\mathrm{Im}}(\omega) = -\mathrm{sgn}(\omega)U_{\mathrm{Re}}(\omega) \tag{20}$$

Therefore, the Hilbert transform changes any even term to an odd term and any odd term to an even term. The Hilbert transforms of harmonic functions are:

$$H[\cos(\omega t)] = \sin(\omega t) \tag{21}$$

$$H[\sin(\omega t)] = -\cos(\omega t) \tag{22}$$

$$H[e^{j\omega t}] = -j\,\mathrm{sgn}(\omega)e^{j\omega t} = \mathrm{sgn}(\omega)e^{j(\omega t - 0.5\pi)} \tag{23}$$

Thus, the Hilbert transform changes any cosine term to a sine term and any sine term to a reversed signed cosine term. Because $\sin(\omega t)=\cos(\omega t-0.5\pi)$ and $-\cos(\omega t)=\sin(\omega t-0.5\pi)$, the Hilbert transformation in the time domain corresponds to a phase lag by -0.5π (or -90°) of all harmonic terms of the Fourier image (spectrum). Using the complex notation of the Fourier transform, the multiplication of the spectral function U(ω) by the

operator -jsgn(ω) provides a 90° phase lag at all positive frequencies and a 90° phase lead at all negative frequencies.

Using what precedes, we can also have the Fourier image of the analytic signal Ψ(t)=u(t)+jv(t) by adding the Fourier transform of each signal:

$$\Psi(t) \xleftrightarrow{F} U(\omega) + j[-j\,\mathrm{sgn}(\omega)U(\omega)] = [1+\mathrm{sgn}(\omega)]U(\omega) \tag{24}$$

$$\text{where } 1+\mathrm{sgn}(\omega) = \begin{cases} 2 & for \omega > 0 \\ 1 & for \omega = 0 \\ 0 & for \omega < 0 \end{cases} \tag{25}$$

Thus the Fourier image of the analytical signal is doubled at positive frequencies and canceled at negative frequencies with respect to U(ω).

In the case of ocean waves, the time-series of the surface elevation can be written with the following notation, which is the Fourier notation:

$$u(t) = \sum_{n=0}^{\infty} a_n \cos(n\sigma t) + b_n \sin(n\sigma t) \tag{26}$$

Where a_n and b_n are the Fourier coefficients of the signal u(t). Using the complex notations, equation (26) is equivalent to:

$$u(t) = \sum_{n=-N}^{N} F(n) e^{jn\sigma t} \tag{27}$$

$$\text{where} \quad F(n) = \begin{cases} \dfrac{a_n - jb_n}{2} & n > 0 \\ 0 & n = 0 \\ \dfrac{a_n + jb_n}{2} & n < 0 \end{cases} \tag{28}$$

To obtain the Fourier coefficients (denoted G(n)) of the Hilbert transform of the signal u(t), we multiply the coefficients of equation (28) by - j sgn(nσ):

$$G(n) = \begin{cases} \dfrac{-ja_n - b_n}{2} & n > 0 \\ 0 & n = 0 \\ \dfrac{ja_n - b_n}{2} & n < 0 \end{cases} \tag{29}$$

Thus the Hilbert transform v(t) of the original time-series can be written as:

$$v(t) = \sum_{n=-N}^{N} G(n) e^{jn\sigma t} = \sum_{n=0}^{N} \frac{-ja_n - b_n}{2} e^{jn\sigma t} + \sum_{n=-N}^{0} \frac{ja_n - b_n}{2} e^{jn\sigma t} \tag{30}$$

Since $a_{-n} = a_n$ and $b_{-n} = b_n$ and by using the change of variables m=-n in the second term of equation (30) we can rewrite v(t) as:

$$v(t)=\sum_{n=0}^{N}[\frac{-ja_n-b_n}{2}e^{jn\sigma t}+\frac{ja_n-b_n}{2}e^{-jn\sigma t}] \tag{31}$$

By reordering the terms of equation (31), we obtain:

$$v(t)=\sum_{n=0}^{N}\frac{ja_n}{2}(-e^{jn\sigma t}+e^{-jn\sigma t})-\frac{b_n}{2}(e^{jn\sigma t}+e^{-jn\sigma t}) \tag{32}$$

which leads to the following notations:

$$v(t)=\sum_{n=0}^{\infty}a_n\sin(n\sigma t)-b_n\cos(n\sigma t) \tag{33}$$

$$v(t)=\sum_{n=1}^{\infty}\sqrt{a_n^2+b_n^2}\cos(n\sigma t-\varepsilon_n-\frac{\pi}{2})=\sum_{n=1}^{\infty}\sqrt{a_n^2+b_n^2}\sin(n\sigma t-\varepsilon_n) \tag{34}$$

where v(t) is the Hilbert transform of the signal u(t) which was written in equation (26) as:

$$u(t)=\sum_{n=0}^{\infty}a_n\cos(n\sigma t)+b_n\sin(n\sigma t)$$

$$u(t)=\sum_{n=1}^{\infty}\sqrt{a_n^2+b_n^2}\cos(n\sigma t-\varepsilon_n) \tag{35}$$

where $\cos(\varepsilon_n) = \frac{a_n}{\sqrt{a_n^2 + b_n^2}}$ and $\sin(\varepsilon_n) = \frac{b_n}{\sqrt{a_n^2 + b_n^2}}$.

This result is restating the fact that sines are transformed into -cosines and cosines are transformed into sines. The pair u(t) and v(t) are obviously very close to each other and we will see in the next paragraph how they are related in the analytic method called the Phase-Time method.

The Phase-Time Method

Traditionally, research on the statistical properties of ocean waves are limited to global quantities and figures, such as the Fourier spectrums, or multiple density functions. These properties give very valuable information about the hydrodynamics of the waves, but the results can not be directly related to an instant time in the original data. *Huang et al.* [1992] presented a new approach using phase information to view and study the properties of frequency modulation, wave group structures, and wave breaking. They applied the Phase-Time Method to ocean wave time-series data and reported the appearance of a new type of wave group. They stated that this method had broad applications to the analysis of time-series data in general.

The Phase-Time Method is a very simple method using the Hilbert transform and phase information to obtain local properties of the frequency of a signal. This method can be described as follows.

Using an elevation time-series record u(t), an analytical function similar to the one defined in equation (13) is constructed:

$$\Psi(t) = u(t) + j\, v(t) \tag{36}$$

where v(t) is the Hilbert transform of the signal u(t) as described in the preceding paragraph.

Figure 6 shows a plot of the two signals u(t) and v(t) for a small time of gauge 1 in experiment 4. We can clearly see the shift of about 90° ($1/4^{th}$ of a peak period).

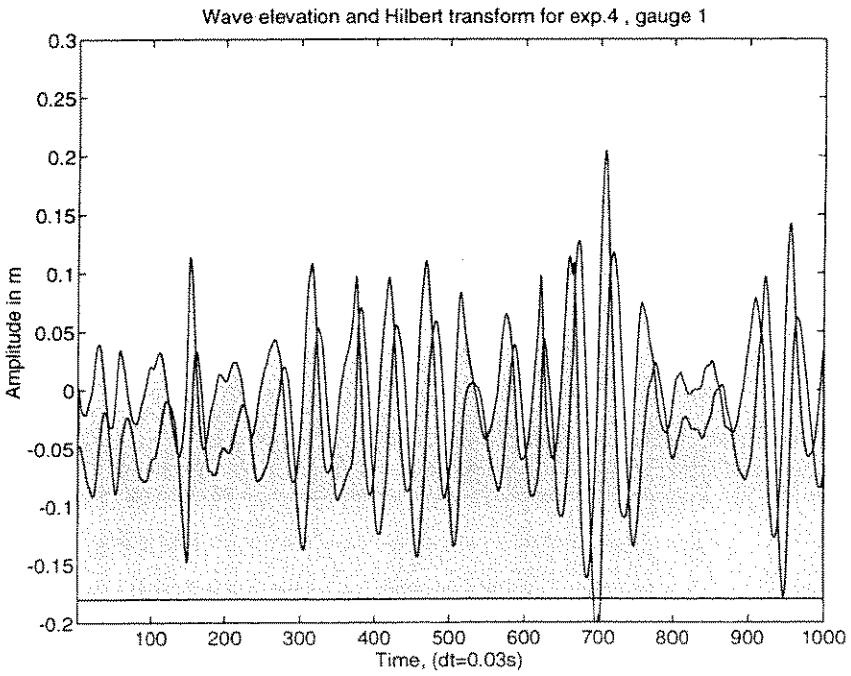

Figure 6. Wave elevation (gray) and Hilbert transform signals.

From this analytic function, we can obtain the phase function Φ(t) defined as:

$$\Phi(t) = \arctan\left(\frac{v(t)}{u(t)}\right) \tag{37}$$

where $\Phi(t)$ can be decomposed into the mean frequency n_0, and a deviation part $\Theta(t)$ in the equation:

$$\Phi(t) = n_0 t + \Theta(t) \tag{38}$$

In the past, many scientists explored some properties of the phase function. *Huang et al.* noted that the association of the phase function with events occurring in real time had never been made and so had the study of local properties of the wave field. They further stated that this phase function was usually wrapped around $\pm\pi$ or between 0 and 2π. The wrapped phase only gives a rather uninformative view of the phase function, since the properties displayed are those of the residue from a given interval ($\pm\pi$ or between 0 and 2π) and not from the data itself. In the Phase-Time Method, the phase is unwrapped in order to obtain a real data related information. Figure 7 shows the unwrapped phase function of the wave data in experiment 4. The slope of the phase function is here of about of 3.65 rad/sec (which higher than the peak frequency F_p).

By detrending the phase function signal (which means subtracting its mean value), we obtain the detailed information on the variable part of the phase angle $\Theta(t)$ (see Figure 8).

By definition, the time derivative of the phase function is the local frequency of the time-series. This means that:

$$F = \frac{\partial \Phi}{\partial t} = n_0 + \frac{\partial \Theta}{\partial t} \tag{39}$$

Therefore, by deriving the signal Θ(t) we obtain the deviation of the frequency from its mean (in a local time domain). Positive and negative values in this derivative will tell that the local frequency is higher or lower than its mean. Figure 9 shows an example of this deviation of local frequency obtained.

This method, to be well executed, has to be used in a data set whose sampling rate is fast enough so that the frequencies of interest are resolved. We will see in the next chapter that the sampling rate is very important in the use of this method.

All the programs used in this research were written with the software and language of Matlab. This method can be applied to wave elevation data with a very simple Matlab sequence that is described in the appendix B.

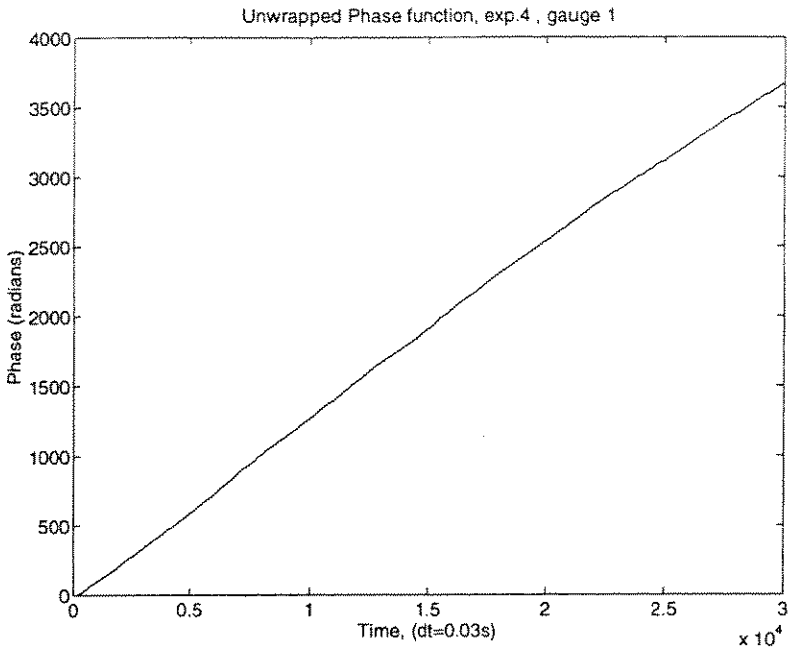

Figure 7. Unwrapped phase function.

Huang et al. described this method as a very useful tool in analyzing wave elevation data, but did not state how to use this method in detecting breaking waves. Also, the limitations and possibilities of this method were not clearly stated by any author who studied the Phase-Time Method. Therefore, we will now explore the possibility of the frequency signal of detecting breaking waves, and show the relations between this signal and the original wave elevation time-series in order to understand the physics of this problem, before the analysis of the data.

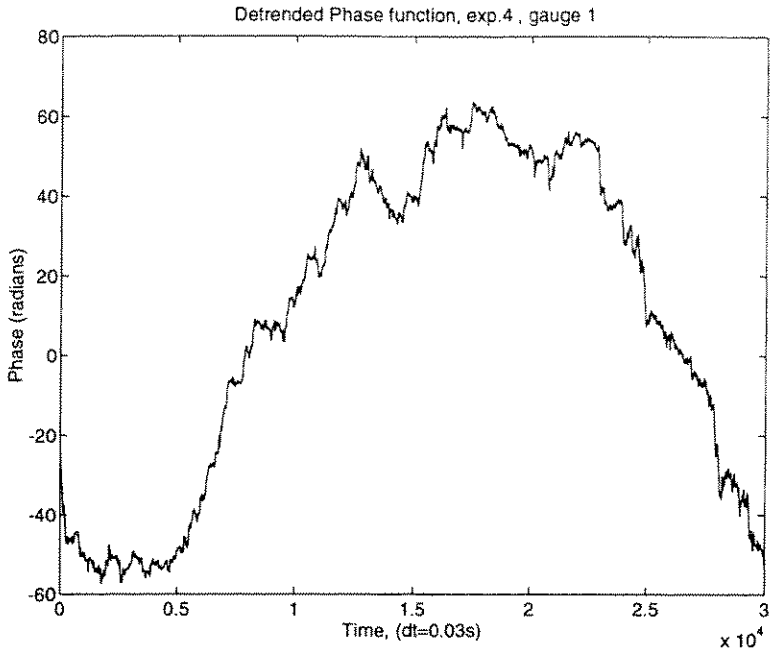

Figure 8. Detrended phase function.

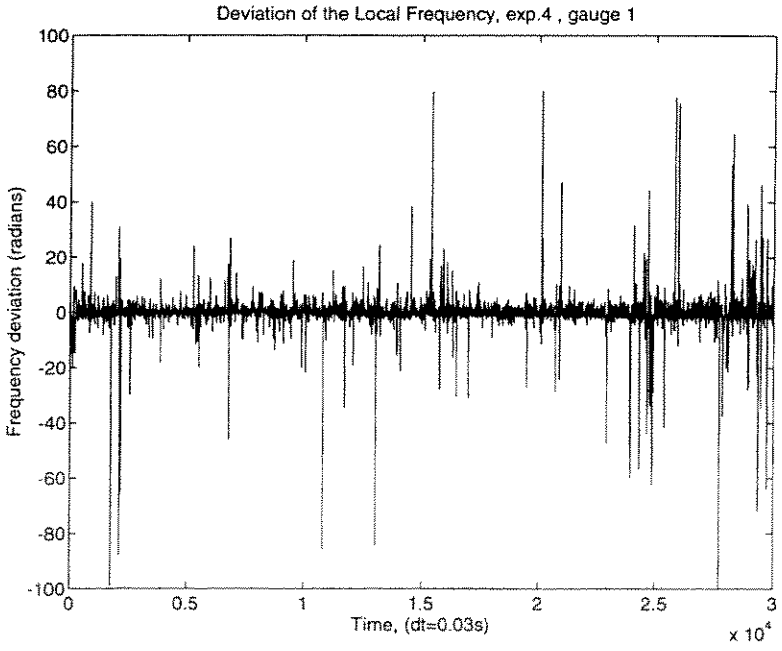

Figure 9. Local frequency deviation.

By using equation (37) and (38) and deriving the phase function directly, we have:

$$F = \frac{\partial \Phi}{\partial t} = \frac{\partial}{\partial t} \arctan(\frac{v(t)}{u(t)}) \tag{40}$$

which can be further developed:

$$F = \frac{\frac{\partial v}{\partial t} u - \frac{\partial u}{\partial t} v}{u^2 + v^2} \tag{41}$$

which provides a considerable information on the properties of this frequency, because u(t) is the wave elevation and v(t) is its Hilbert transform. This also allows us to understand the physics of this frequency signal.

By looking at equation (41) we can draw several conclusions on the behavior of this local frequency signal.

Firstly we can look at the characteristics of breaking waves in the ocean. We know that the breaking will occur only if the height of the wave is large. Breaking will occur at the top of the wave, were $\frac{\partial u}{\partial t}$ is almost zero and v(t) is very small (because of the 90° shift). Therefore v at this instant will be negligible compared to u. Therefore when breaking is occurring, v<<u and the second term in equation (41) is negligible compared to the first term. Therefore, for waves that are possibly breaking, and at the top of the wave, we have:

$$F = \frac{\frac{\partial v}{\partial t}}{u} \tag{42}$$

This frequency is related to the deviation of the Hilbert transform of the original wave elevation time-series. The frequency will have a deviation only if $\frac{\partial v}{\partial t}$ increases at this moment.

Using the notations of equation (26) and (33) we can develop this frequency as follows:

$$F = \frac{\frac{\partial v}{\partial t}}{u} = \frac{\sum_{n=0}^{\infty} a_n(n\sigma)\cos(n\sigma t) + b_n(n\sigma)\sin(n\sigma t)}{\sum_{n=0}^{\infty} a_n \cos(n\sigma t) + b_n \sin(n\sigma t)} \tag{43}$$

We can notice that if the time-series contains only one term in cosines or sine, then F=nσ which is the mean frequency. There is no deviation for regular and periodic signals of only one frequency.

Since cosine and sine are always <=1, when nσ>>1 which means when we have high frequency waves, the numerator of equation (43) is much larger than the denominator, and the frequency deviation is thus high. This certainly agrees with the fact that breaking occurs in the ocean when a multitude of high frequency waves build on top of a long wave and allow the energy to concentrate, until the breaking appears.

Now, we can notice that when u(t) is close to zero, then we can have

$$F \cong \frac{-\frac{\partial u}{\partial t}}{v} \tag{44}$$

Therefore, in some cases like two close frequency waves, where v tends to zero too, then the deviation of the frequency will be very high. This problem of having $u^2 + v^2$ as the denominator will result in huge peaks of deviation (50 to 100 radians) at certain times in the wave elevation record where the wave elevation and its Hilbert transform are close to zero (see Figure 10).

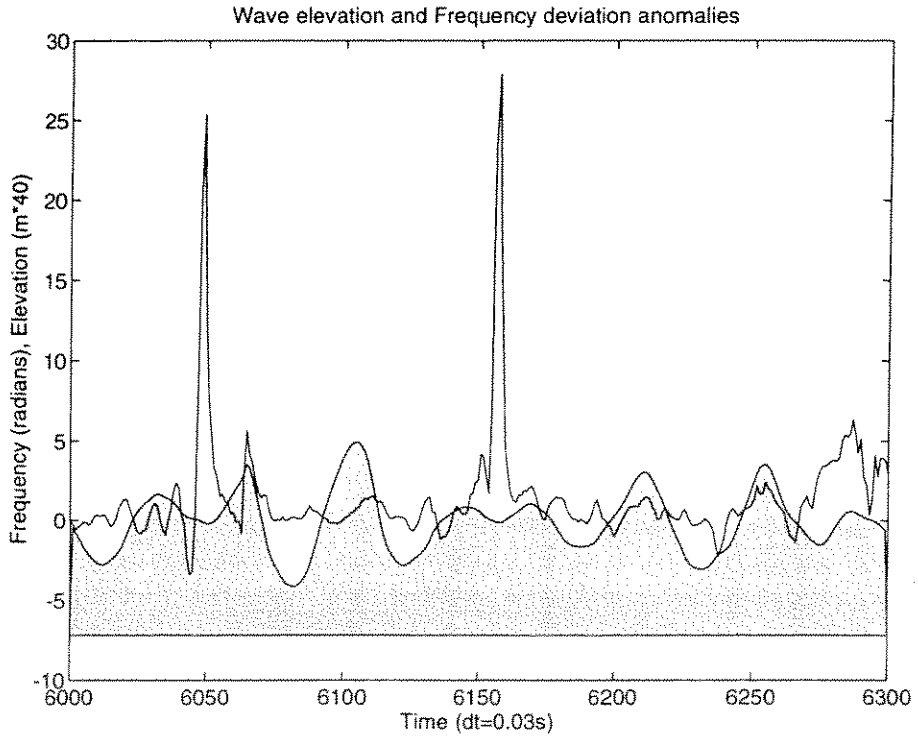

Figure 10. Local frequency deviation when the wave elevation is close to zero.

This problem really limits the power of the Phase-Time method and will greatly diminish the possibilities of using the frequency as a detection signal. This noise has to be eliminated before using the frequency signal in the breaking detection. That is why a parameter must be found to filter the frequency signal and make it useful. We will see in the next chapter that the wave height is a simple and very efficient parameter to realize this objective.

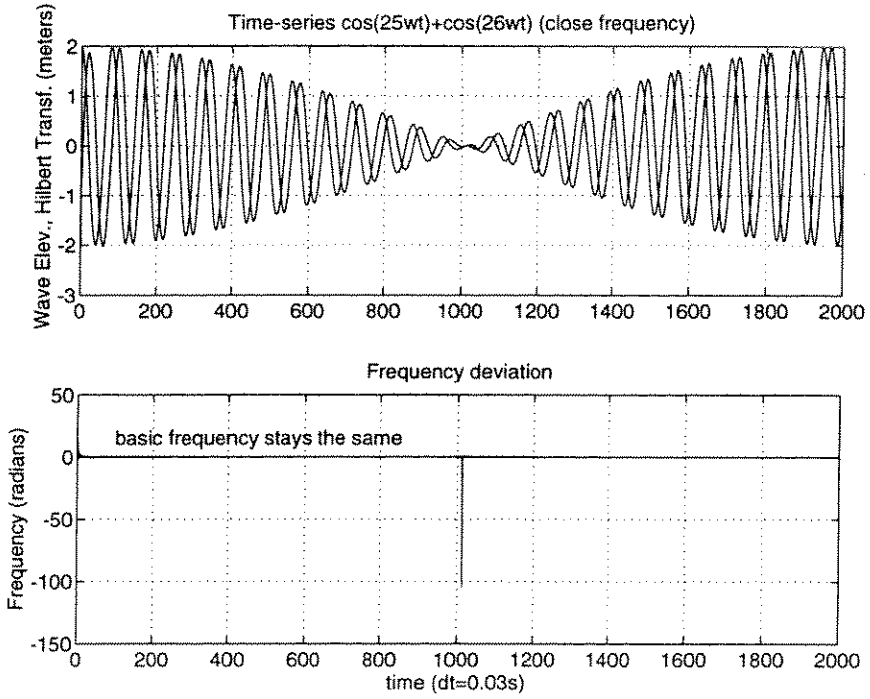

Figure 11. Close frequency waves (cos(25ωt)+cos(26ωt)).

Figure 11 and 12 show the frequency deviation signal obtained for two types of waves, one consisting of the addition of 2 waves close in frequency ($\cos(25\omega t)+\cos(26\omega t)$), and the second one of two waves with real different

frequencies ($\cos(25\omega t)+\frac{1}{2}\cos(50\omega t)$). On these two simple examples , it can be seen that the decreases in frequency occur when the elevation signal or its Hilbert transform are close or equal to zero. This confirms the conclusions drawn above.

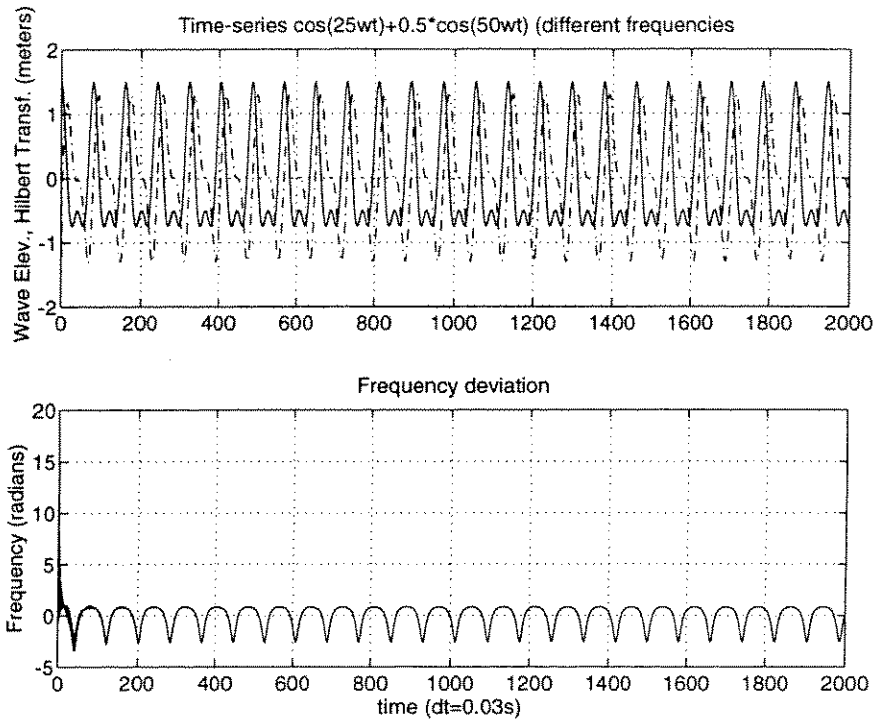

Figure 12. Different frequencies waves (cos(25ωt)+1/2 cos(50ωt)).

CHAPTER IV

DETECTION MODEL

This chapter describes the data analysis and the construction of a simple and efficient model to detect the breaking waves in the deep water. Many parameters have been studied and tested as a tool of detection with various results. The data analysis, the use of video documentation, and the comparison with other research results, will be described in this chapter.

Video documentation

All experiments were recorded using 2 cameras focused on the 11 gauge array whose output was then recorded side-by-side as a single video image. The implementation of the video documentation was critical to this study because it allowed a visual determination of each breaking events. A picture of an actual breaking wave going through the first five gauges taken from the video can be seen in Figure 13.

The first step of the analysis was to match the video recordings of the experiments with the actual data consisting of matrices of the elevation records for each gauge in each experiment. For each of these experiments, the data file consists of 32700 data points for each gauge (the sampling rate being 0.03 seconds per data point, 32700 data points corresponds to about 16 min of measurements). With the random movements of the panels of the wave maker and the possible periodic sequence of waves propagated in the

basin, it is almost impossible to match exactly the data set with the actual video record displayed on a television. Even if the elevation record can be displayed using a Matlab program, the possibility of mismatching a wave from the data record with a wave of the video record is very high. That is the reasoning behind the implementation of a means of showing when the data acquisition had begun on the video. In fact, after a few seconds of data acquisition, an electrical signal would light an electric bulb positioned on the gauge array. This in turn would allow a visual detection of the electrical signal on the videotape. A simple Matlab program gave us the exact data point of the beginning of this electrical signal, allowing the matching of the data points recorded with the video documentation (see Table 3). This process was implemented after the third experiment and the first 3 experiments do not have any matching system.

Figure 13. Video documentation (breaking wave going through the first gauges).

Table 3. Electrical Signal for the Experiments

Exp. #	Tape Start	Light on	Tape Light on	Light off	Tape Light off
wt1	16:30'29"	-	-	-	-
wt2	17:37'29"	-	-	-	-
wt3	18:17'11"	-	-	-	-
wt4	14:00'44"	217	14:00'57"+03	32588	14:17'08"
wt4_2	16:16'08"	193	16:16'40"+08	32516	16:32'50"
wt5	14:48'21"	349	14:48'32"+22	32487	15:04'37"
wt6	08:40'13"	727	08:40'24"+07	32511	08:56'19"
wt6_2	10:45'06"	185	10:45'41"+00	32511	11:01'50"
wt7	09:33'53"	337	09:34'29"+14	32634	09:50'38"
wt8	11:40'04"	154	11:40'41"+08	32490	11:56'51"
wt9	13:12'08"	151	13:12'41"+02	32511	13:28'51"
wt10	14:30'19"	154	14:30'53"+07	32507	14:47'03"

dt = 0.03s

The next step was to watch the video record of every experiment and identify every wave breaking event. For every experiment, the time for each breaking wave on the video record was noted and the numbers of the gauges where the wave breaking occurred were recorded. In addition, an evaluation was made regarding the intensity of the breaking. Therefore if breaking occurs, the gauges concerned will be annotated with a code as described below:

-I : either when the wave is beginning to break, or when the wave is breaking with a very small amount of white capping on top of the wave.

-S : when the wave is fully breaking with a small vertical motion and a small amount of white capping coming from the breaking at this gauge.

-M : when the wave is breaking and spilling leaving a large amount of white capping in front or on top of the breaking wave.

-L : when the breaking event is intense, and the wave has a large and very visual change in shape, looking like a plunging breaker. The white capping and the vertical motion of the wave itself are very pronounced for this type of breaker. This "L" code denotes the most intense breaking events in the wave data record.

Using this type of categorical distinction, each experiment was studied and each breaking wave recorded to allow the analysis of the actual wave elevation data (See Appendix A).

Data analysis

The entire data analysis, and all programming have been accomplished using Matlab software, which allows the computation of very large matrices and excellent visualization possibilities. One of the main program used for this research is listed in Appendix C.

It is clear that there is no existing methodology to identify the breaking events just by examining the wave elevation record. If it is true that the breaking waves will usually correspond to maximum wave heights and sharp crests on the wave elevation record, it is literally impossible to identify these breaking events just by looking at the elevation record. That is why the Phase-Time Method is studied here in order to facilitate the detection of breaking events in a wave elevation record.

The first operation was to plot the wave elevation record and the Hilbert frequency obtained in the Phase-Time Method on the same graphs and to mark the